Journal of Chromatography A, 1320 (2013) 48–65

Contents lists available at ScienceDirect

Journal of Chromatography A

journal homepage: www.elsevier.com/locate/chroma

Quadruple parallel mass spectrometry for analysis of vitamin D and triacylglycerols in a dietary supplement

William Craig Byrdwell*

USDA, Agricultural Research Service, Beltsville Human Nutrition Research Center, Food Composition and Methods Development Laboratory, USA

ARTICLE INFO

Article history:
Received 26 April 2013
Received in revised form
24 September 2013
Accepted 9 October 2013
Available online 18 October 2013

Keywords:
Vitamin D
Cholecalciferol
Triacylglycerols
APCI-MS
ESI-MS
APPI-MS

ABSTRACT

A "dilute-and-shoot" method for vitamin D and triacylglycerols is demonstrated that employed four mass spectrometers, operating in different ionization modes, for a "quadruple parallel mass spectrometry" analysis, plus three other detectors, for seven detectors overall. Sets of five samples of dietary supplement gelcaps labeled to contain 25.0 μg (1000 International Units, IU) vitamin D_3 in olive oil were diluted to 100 mL and analyzed in triplicate by atmospheric pressure chemical ionization (APCI) mass spectrometry (MS), atmospheric pressure photoionization (APPI) MS and electrospray ionization (ESI) MS, along with an ultraviolet (UV) detector, corona charged aerosol detector (CAD), and an evaporative light scattering detector (ELSD), simultaneously in parallel. UV detection allowed calculation by internal standard (IS), external standard (ES), and response factor (RF) approaches, which gave values of 0.2861 ± 0.0044, 0.2870 ± 0.0059, and 0.2857 ± 0.0042 μg/mL, respectively, which were not statistically significantly different. This indicated an average amount of vitamin D_3 of 14.5% over the label amount. APCI-MS analysis by selected ion monitoring (SIM) and two transitions of selected reaction monitoring (SRM) provided values of 0.2849± 0.0055, 0.2885± 0.0090, and 0.2939 ± 0.0097 μg/mL, respectively, relative to vitamin D_2 as the IS. The triacylglycerol (TAG) composition was determined by APCI-MS, APPI-MS and ESI-MS, and the fatty acid (FA) compositions calculated from the TAG compositions were compared to the FA composition determined by gas chromatography (GC) with flame ionization detection (FID) of the FA methyl esters (FAME). APCI-MS provided the FA composition closest to that determined by GC-FID of the FAME. A previously reported approach to TAG response factor calculation was employed, which brought all TAG compositions into good agreement with each other, and the calculated FA compositions into excellent agreement with the FA composition determined from GC-FID of the FAME.

Published by Elsevier B.V.

1. Introduction

Cholecalciferol, vitamin D_3, and ergocalciferol, vitamin D_2, continue to be of interest to researchers and consumers alike, due to the fact that study after study has appeared that indicates deleterious effects of dietary deficiency in this vitamin, collectively referred to as vitamin D. While these two components are the forms of the vitamin normally consumed, it is the 25-hydroxy vitamin D metabolite formed in the liver (and elsewhere) that acts as the primary biomarker for the nutrient. Because of structural differences between the native molecules and their circulating metabolites, and differences in sample matrices between vitamin D-containing foods and biological fluids such as serum, which are used to assess its biological adequacy, the methods for analysis of the dietary form of the nutrient are often very different from those used to quantify its metabolite(s).

Biological samples can be quickly and routinely analyzed using radioimmunoassays (RIA) or competitive protein binding assays (CPBA), although lack of specificity leading to cross-reaction between forms of the metabolites and other issues makes these types of analysis less than ideal, but nevertheless useful for high throughput clinical screening. For foods and supplements, on the other hand, vitamin D is the analyte, and an entirely different approach is used. For analysis with the greatest level of specificity and high sensitivity, liquid chromatography with mass spectrometric detection is used. LC-MS is usually considered the "gold-standard" for vitamin D analysis due to its ability to use specific precursor-product fragmentation pathways in selected reaction monitoring (SRM) experiments to differentiate forms of the nutrient and its metabolites.

The coupling of liquid chromatography to mass spectrometry is accomplished nowadays using atmospheric pressure ionization (API) interfaces, the most common of which are atmospheric pressure chemical ionization (APCI), electrospray ionization (ESI), and atmospheric pressure photoionization (APPI). Vitamin D, however, does not respond well to ESI, so APCI has become the preferred

* Tel.: +301 504 9357; fax: +301 504 8314.
E-mail address: C.Byrdwell@ars.usda.gov

0021-9673/$ – see front matter. Published by Elsevier B.V.
http://dx.doi.org/10.1016/j.chroma.2013.10.031

ionization technique for LC-MS of vitamin D. Only very limited reports are available describing the use of APPI-MS for vitamin D analysis [1,2], since this is not the default source supplied with most mass spectrometers. Furthermore, although a few classes of molecules respond better to APPI than APCI, APCI is more of a universal ionization technique, since a very wide range of classes of molecules respond well to this ionization process, without the need for the addition of dopant, normally associated with APPI.

Prior to LC-MS analysis, extensive sample extraction and cleanup procedures are still generally required before samples are ready for the final chromatographic separation and analysis. In 1999, Eitenmiller and Landen [3] summarized the methods commonly used at that time, and similar approaches continue to be used today. Advances in LC have led to the use of ultra-high performance liquid chromatography (UHPLC) for the chromatographic separation [4–6], but preliminary sample preparation often continues to employ various combinations of saponification and either liquid/liquid extraction (LLE) or solid phase extraction (SPE) prior to analysis. Unfortunately, these sample preparation steps are often the most labor-intensive part of the analytical process. While automated SPE equipment is commercially available and is used in some cases, only a fraction of the methods describing LC-MS of vitamin D employ automated sample preparation. Thus, while great advancements have been made in LC and MS instrumentation, especially in regard to increased mass spectrometer sensitivity, the sample preparation steps often still require substantial commitments of time and expertise by qualified chemical technicians.

To address the issue of saponification and extraction, we recently reported a "dilute-and-shoot" approach that eliminated the saponification and extraction steps altogether, giving greatly simplified sample preparation [7]. While this approach is not applicable to all sample types, for those samples to which it does apply, it allows a substantial reduction in sample preparation time and chemical resources used. Of equal importance is the fact that components in the sample that were previously regarded as interfering species, such as triacylglycerols (TAG) that required isolation and removal, are now able to be analyzed along with the vitamin D analyte. This allows a holistic analysis of the entire samples, instead of targeted analysis of a single analyte to the exclusion of other components.

Since many components are analyzed using such an approach, it is beneficial to employ multiple ionization techniques, because some classes of compounds respond better to different types of ionization, and different ionization techniques provide different types of mass spectra. Specifically, ESI produces mainly molecular adduct ions from TAG, with the addition of a suitable electrolyte, which are ideal for further structural characterization by MS^n, whereas APCI usually produces substantial diacylglycerol-like fragments, $[DAG]^+$, that provide an immediate indication of the constituent fatty acids making up the TAG, while at the same time yielding varying amounts of intact protonated molecule, $[M+H]^+$, depending on the degree of unsaturation in the TAG. APPI can also be used for TAG analysis [8–13], and gives spectra that appear similar to spectra obtained by APCI-MS. In order to compare the results obtained by these disparate ionization techniques, many reports have demonstrated analysis of the same samples using different combinations of these ionization sources, almost always by sequentially re-analyzing samples after changing the ionization source between runs. A database search of "mass spectrometry" and "APPI" and "APCI" returns 100 citations, a search of "mass spectrometry" and "APPI" and "ESI" returns 102 citations, and a search of "mass spectrometry" and "APCI" and "ESI" returns 450 citations! Including APPI, APCI and ESI together produces 64 citations, but only 4 seem to be applications to lipids or triacylglycerols (found by including ("lipid*" or "triacylglycerol*" or "triglyceride*") as keywords) [9,13–15]. Clearly there is substantial interest in acquisition of data from two or more ionization techniques in order to obtain the complementary information that these API methods provide. Obviously there are too many citations to list here, even though these searches are not comprehensive.

Very few reports, on the other hand, have employed a "parallel mass spectrometry" approach, in which two or three mass spectrometers, as well as other detectors, have been attached in parallel to the same effluent stream [16,17,7,18,19]. In addition to allowing a direct comparison between ionization types, this approach reduces the number of runs necessary to acquire the complementary data, and eliminates all run-to-run variability in chromatographic runs, which can complicate interpretation of the data from complex samples.

Described here is the first report of four mass spectrometers in parallel, for a "quadruple parallel mass spectrometry" experiment, also in parallel with a UV detector, evaporative light scattering detector (ELSD), and corona charged aerosol detector (CAD), for seven detectors overall. ESI-MS, APPI-MS, and high- and low-sensitivity APCI-MS are used for a holistic analysis of dietary supplements containing olive oil and vitamin D using a dilute-and-shoot approach. A new meta-analysis of sample results over two months using numerous methods for quantification is presented. We also incorporate, for the first time, the $1 \times {}^{13}C$ isotopic variant for TAG analysis to increase signal, without loss of specificity. This work also provides the first report of the application of a previously reported approach to determining response factors from GC with flame ionization detection (FID) to APPI-MS of TAG. Finally, we demonstrate a novel modification of the previously reported approach to compensate for charge saturation in ESI-MS.

2. Materials and methods

2.1. Chemicals and samples

Fisher Optima LC-MS grade methanol (MeOH), #A456-4, and acetonitrile (ACN), #A955-4, were used (Fisher Scientific, Pittsburgh, PA, USA). Fisher Optima grade methylene chloride (dichloromethane, DCM), #D151-4, was used. The following solvents and reagents were obtained from Sigma-Aldrich Co. (St. Louis, MO, USA): ammonium formate #516961, synthetic crystalline cholecalciferol #1357, synthetic crystalline ergocalciferol #5750, boron trifluoride 14% in methanol, and ACS reagent grade sodium chloride and sodium hydroxide. GC fatty acid methyl ester (FAME) reference standards GLC-68B, GLC-68D, GLC-14B, and methyl tricosanoate (C23:0) were obtained from Nu-Chek Prep (Elysian, MN, USA). Methyl pentacosanoate (C25:0) was from Santa Cruz Biotechnology (Dallas, TX, USA), and methyl hexacosanoate (26:0) was from Matreya, LLC (Pleasant Gap, PA, USA). Deionized (D.I.) water was obtained from a Millipore Milli-Q® purification system (Millipore, Bedford, MA, USA).

Dietary supplement gelcaps containing 25 μg, or 1000 International Units (IU), vitamin D_3 in olive oil, with the vitamin D_3 from lanolin, were ordered from an online supplier of vitamins. Samples were received on 1/19/2010 unrefrigerated, and were stored refrigerated upon receipt, as would be typical for the average consumer. Sample weights for the primary samples used in this report were 0.10524 g, 0.10414 g, 0.09610 g, 0.10191 g, 0.10288 g, for an average of 0.10212 ± 0.00343 g (3.36% RSD). Gelcap samples were prepared and bracketed sequences were run as previously described [7].

2.2. Instrumentation

2.2.1. High performance liquid chromatography

The HPLC conditions, solvent gradient, and parameters, including those for the DAD, ELSD, and CAD have been described

recently [7] and are provided in Supplemental Materials for convenience. After the DAD, a series of five Valco tees was used to split the flow to go to: 1) the APPI-MS mass spectrometer, 2) corona CAD, 3) ELSD, 4) APCI-MS mass spectrometer in full scan mode, 5) ESI-MS mass spectrometer, and 6) an APCI-MS mass spectrometer in selected ion monitoring (SIM), SRM and full scan modes. The flow to each instrument was dictated primarily by the length and internal diameter of the fused silica tubing leading from the tee to the instrument. Compared to our earlier report [7], an additional tee was inserted between the third and fourth tees, to which was attached a ~248 cm piece of 100 μm i.d. fused silica tubing, and the perpendicular port of the now fifth tee was changed to a ~93 cm piece of 75 μm i.d. fused silica tubing, to reduce the flow rate to the ESI-MS instrument, and the tubing to the corona CAD (2nd tee) was reduced to 75 μm to reduce flow to the new corona Ultra RS CAD. The lengths and flow rates (average of $n = 3$ determinations) of the new configuration of tees was as follows (p = perpendicular port, s = straight-through port): 1(p) 188 cm of 100 μm (198 μL/min = 16.1%); 2(p) 123 cm of 75 μm (92 μL/min = 7.5%); 3(p) 125 cm of 100 μm (292 μL/min = 23.9%); 4(p) 248 cm of 100 μm (145 μL/min = 11.9%); 5(p) 93 cm of 75 μm (121 μL/min = 9.9%); 5(s) 93 cm of 100 μm (376 μL/min = 30.7%).

2.2.2. Mass spectrometry

Different instruments, used in a different configuration, were used for this analysis compared to our "triple parallel mass spectrometry" report.[7] For analysis of TAG in this and future reports, the QTrap 5500 hybrid mass spectrometer was exchanged for a QTrap 4000 hybrid mass spectrometer, which offered a higher upper mass limit (up to *m/z* 2800) but lower sensitivity. For the current experiments, the QTrap 4000 was operated in ESI-MS mode, whereas a TSQ Vantage EMR (extended mass range) was used for APCI-MS to conduct sensitive quantification of vitamin D (and TAG), using the same modes as previously used on the QTrap 5500 (SIM, SRM1, and SRM2). The LCQ Deca XP ion trap mass spectrometer was used for APPI-MS^3 in these experiments, versus ESI-MS^4 in the previous report. MS^4 was reduced to MS^3 because TAG produced few productive MS^4 spectra, and used valuable duty cycle time. The TSQ 7000 was used in the same capacity as previously reported. Only very simple modification of the 12-switch contact closure distribution manifold was required to send the contact closures to the two new instruments (QTrap 4000 and TSQ Vantage EMR).

2.2.2.1. APCI-MS for vitamin D_3 and TAG. Flow from the straight port of the fifth splitting tee went to a TSQ Vantage EMR mass spectrometer (ThermoScientific, San Jose, CA, USA) controlled by Xcalibur® 2.1. The instrumental method used for calibration standards contained one time segment of 28 min, while samples employed two time segments, the first was 28 min with the same conditions used for the standards, and the second was 102 min. The first segment was used to compare SIM, and two transitions of SRM, plus full-scan acquisition from *m/z* 200-2000, with a 1.0 s scan time. The instrument was operated in APCI mode, using a vaporizer temperature of 400 °C, heated capillary at 265 °C, corona current at 4.0 μA, sheath gas at 50 arbitrary units (a.u.) and auxiliary gas at 5 a.u. For SIM, *m/z* 379.3 (=$[M+H-H_2O]^+$) and *m/z* 397.3 (=$[M+H]^+$) were used for vitamin D_2 and *m/z* 367.3 (=$[M+H-H_2O]^+$) and *m/z* 385.3 (=$[M+H]^+$) were used for vitamin D_3, all with a peak width of 1.0 and scan time of 0.5 s. For SRM, the first pair of transitions was *m/z* 397.3 → *m/z* 379.3 and *m/z* 385.3 → *m/z* 367.3 for vitamin D_2 and D_3, respectively. A second pair of transitions used was *m/z* 397.3 → *m/z* 271.2 and *m/z* 385.3 → *m/z* 259.2 for vitamin D_2 and D_3. All SRM scans used a peak width of 1.0, a scan time of 0.5 s, and collision energy of 15 V, which minimized low-mass fragment production. The second time segment, used for TAG analysis, performed a full scan from *m/z* 200 to 2000, with a 1.5 s scan time, followed by data dependent acquisition (auto-MS/MS) of the most intense ion over *m/z* 300 from the full scan, using a scan time of 1.0 s and collision energy of 30 V, optimized for TAG. The 70 min column cleanup run used a scan range of *m/z* 200–3000 with a scan time of 1.5 s followed by one data dependant scan, using a scan time of 1.0 s and collision energy of 30 V.

2.2.2.2. ESI-MS for TAG. Flow from the perpendicular outlet of the fifth tee was directed to a QTrap 4000 mass spectrometer (AB Sciex, Foster City, CA, USA), using Analyst® 1.5.2, operated in positive ESI mode. The curtain gas was optimized at 30 a.u., sheath gas (GS1) at 25 a.u., auxiliary gas (GS2) at 0 a.u., the temperature was 100 °C, and spray voltage at 5 kV. Scans were obtained from *m/z* 200 to 2000, with a scan time of 2.0 s. Data dependant acquisition was used to obtain MS/MS spectra from the two most abundant ions above *m/z* 300, using a medium gas setting and 40 V collision energy. 50 mM ammonium formate electrolyte solution (see Supplemental Materials) was supplied via the perpendicular branch of a tee connected to source inlet, at a flow rate of 40 μL/min from an ABI 140B solvent delivery module (Applied Biosystems, Foster City, CA, USA), using a contact closure to coordinate refilling syringes during the 5 min LC dead volume. An HP 1050 pumping D.I. water at 0.1 mL/min was used to flush the source between runs. The ABI 140B and HP 1050 were plumbed through the electronic switching valve on the front of the LCQ Deca XP to provide a D.I. water source rinse between runs, including the column dead time, since the QTrap did not have an electronic switching valve (see plumbing diagram in supplementary materials to previous report [7]).

2.2.2.3. APCI-MS for TAG. The perpendicular outlet of the fourth splitting tee went to a TSQ 7000 tandem sector quadrupole mass spectrometer (ThermoElectron Corp., San Jose, CA, USA), using XCalibur® 1.1, operated in positive full-scan APCI mode. The vaporizer heater was operated at 400 °C, the capillary heater was at 265 °C, the corona discharge current was 4.0 μA, and sheath and auxiliary gases were set to 35 psi and 10 (arbitrary units, a.u.), respectively. Scans were recorded from *m/z* 150–1950 in 2 s.

2.2.2.4. LCQ Deca XP for APPI-MS. Flow from the perpendicular outlet of the first tee went to a tee attached to the inlet of an APPI/APCI combination source (Morpho Detection, Inc., formerly Syagen Technologies, Inc., Tustin, CA) mounted on the LCQ Deca XP mass spectrometer (ThermoElectron Corp., San Jose, CA, USA), which was operated in APPI-only mode (corona needle removed). Attached to the perpendicular branch of the source inlet tee was a line from an Agilent 1290 UHPLC pump operated at 40 μL/min to provide acetone as the dopant. The vaporizer heater was at 400 °C, the sheath and auxiliary gases were set to 50 and 30 a.u., respectively, and the capillary temperature was 265 °C. Full-scan spectra were acquired from *m/z* 200 to 2000 in 2.0 s for all runs. Auto-MS/MS and auto-MS^3 scans used an activation *q* of 0.35 at a normalized collision energy of 50%, with an activation time of 900 ms and an isolation width of 2.0.

2.2.3. GC-FID

AOCS method Ce-1b-89 was used with minor modification to accommodate the very long chain fatty acid (VLCFA) methyl esters. A higher final temperature (250 °C) was used, 20 mg of samples were used, and the absolute quantification of docosahexaenoic acid (DHA) and eicosapentaenoic acid (EPA) was not performed. The gas chromatograph was an Agilent Technologies 6890 N (Santa Clara, CA, USA) with 7683 Series injector, split/splitless inlet (operated split mode, 1:50), and using GC Chemstation software (Rev. A.10.02). An omegawax™ 250 column (30 m × 0.25 mm i.d. × 0.25 μm film) (Supelco, Inc., Bellefonte, PA, USA) was used

with an initial temperature of 170 °C, a gradient of 1 °C/min to 250 °C, and 0 min initial and final hold times. Helium carrier gas was used at a flow rate of 1 mL/min. The inlet was at 250 °C and the FID was at 270 °C, with hydrogen flow at 45 mL/min, air flow at 450 mL/min, and helium make-up gas flow at 45 mL/min.

Standards mixture GLC-68B was used to produce response factors (RF) for FAME quantification by GC-FID. Other pure FAME standards and mixtures GLC-68D and GLC-14B were used for identification of retention times of FAME not in GLC-68B, such as saturated odd-chain FAME and VLCFAME. RF for C21:0 and C23:0 FAME were estimated from the average of the RF of the surrounding two even-chain FAME in GLC-68B, and FAME greater than C24:0 used the RF for 24:0. VLCFA were present at such low levels this introduced minimal uncertainty into the analyses.

2.2.4. Calculations

All peak areas were manually integrated using: 1) Agilent Chemstation software for UV at 265 nm and 210 nm for vitamin D_2 and D_3; 2) Xcalibur 2.1.0 on the TSQ Vantage EMR for MS, SIM, SRM1 and SRM2 for vitamin D_2 and D_3, and for EIC of TAG; 3) Analyst 1.5.2 for the QTrap 4000 ESI-MS EIC of TAG; 4) Xcalibur 1.3 on the LCQ Deca XP for the APPI-MS EIC of TAG; and 5) Xcalibur 1.2 on the TSQ 7000 for the EIC of TAG.

Integration of peaks used grouped EIC, produced by specifying all ions associated with a particular TAG in the processing method, so that all specified ions were extracted together as a group for each TAG and DAG. This has the advantage of producing much cleaner chromatograms, since noise was minimized and extraneous peaks were not included. It is not as thorough, however, as extracting every individual ion chromatogram separately and integrating the peaks therein. When extracted separately, those data allow facile calculation of ratios of fragments that can be used for regioisomer determination, and the ratios can be used to reconstruct the raw mass spectra [20]. However, that approach is much more time consuming, since each peak in every ion chromatogram must be separately integrated.

One other modification to our normal method for TAG quantification was employed. In the group EIC chromatogram mass lists used for quantification of APCI-MS and APPI-MS, the first ^{13}C isotopic peaks were included to increase the amount of signal and therefore the sensitivity. Since TAG differ by an integer number of double bonds or by carbon chain length, they almost always differ by at least 2 amu. Thus, $1 \times {}^{13}C$ isotope, at one mass unit higher, does not overlap other species, and shows the same profile as the monoisotopic peak (demonstrated below). Thus, for a typical ion that has a $1 \times {}^{13}C$ abundance of 30% to 60% (depending on whether it is a $[DAG]^+$, or $[M+H]^+$), the overall signal, and therefore the integrated area, can be increased with no loss of specificity.

The integrated areas for each gelcap were divided by the oil weight of that gelcap, and multiplied by the average weight for that set, so that all gelcaps within a set were compared on an equal weight basis, referred to as sample weight normalized results.

Sample weights were obtained to five significant figures, but vitamin D_3 values herein are presented only to the second uncertain figure or to 0.0001 μg/mL, whichever is greater. TAG and FA percentage compositions are given to 0.01%, as typical in the literature.

The following abbreviations are used for TAG analysis (C:db, carbons:double bonds): myristic acyl chain (a.c.), M, 14:0; palmitoleic a.c., Po, 16:1; palmitic a.c., P, 16:0; linolenic a.c., Ln, 18:3; linoleic a.c., L, 18:2; oleic a.c., O, 18:1; stearic a.c., S, 18:0; gadoleic a.c., Ga, 20:1; arachidic a.c., A, 20:0; behenic a.c., B, 22:0; lignoceric a.c., Lg, 24:0; cerotic a.c., Ce, 26:0; others, not abbreviated: 21:0, 23:0, 25:0.

Table 1
Sample weight normalized amounts of vitamin D_3, in μg/mL, for gelcap contents diluted to 100 mL, determined by ultraviolet (UV) detection. Results by internal standard (IS), external standard (ES), and internal standard response factor (iRF) approaches, relative to vitamin D_2 internal standard (0.500 μg/mL = 2000 IU/100 mL).

UV at 265 nm		
IS ± SD	ES ± SD	iRF[b] ± SD
0.2895[a] ± 0.0024	0.2913 ± 0.0042	0.2889 ± 0.0023
0.2894 ± 0.0079	0.2927 ± 0.0071	0.2888 ± 0.0076
0.2830 ± 0.0031	0.2863 ± 0.0011	0.2826 ± 0.0030
0.2888 ± 0.0018	0.2871 ± 0.0009	0.2883 ± 0.0018
0.2800 ± 0.0088	0.2776 ± 0.0055	0.2798 ± 0.0085
Avg. 0.2861 ± 0.0044	0.2870 ± 0.0059	0.2857 ± 0.0042
±0.013[c]	±0.010	±0.012
1145[d] ± 17	1148 ± 24	1143 ± 17
UV at 210 nm		
IS ± SD	ES ± SD	iRF[b] ± SD
0.254[a] ± 0.061	0.260 ± 0.058	0.252 ± 0.053
0.286 ± 0.019	0.298 ± 0.020	0.279 ± 0.016
0.282 ± 0.021	0.2740 ± 0.0092	0.276 ± 0.019
0.303 ± 0.033	0.2952 ± 0.0081	0.294 ± 0.028
0.278 ± 0.027	0.283 ± 0.012	0.273 ± 0.024
Avg. 0.281 ± 0.017	0.282 ± 0.016	0.275 ± 0.015
±0.080[c]	±0.063	±0.069
1123[d] ± 70	1129 ± 63	1098 ± 60

[a] Values and uncertainties are given to 0.0001 μg/mL, or to the second uncertain figure.
[b] Response factor calculated using ratio of 0.25 μg/mL standard to internal standard.
[c] Square root of the sum of the squares of the individual standard deviations.
[d] Per capsule average values in International Units, IU, where 1 IU = 0.025 μg.

3. Results and discussion

All samples dissolved completely in the dilution solvent, which eliminated all issues related to losses during wet chemical treatment (e.g., saponification), liquid–liquid extraction efficiency, and other issues associated with conventional analyses that involve saponification and extraction.

During development of the MS quadruple parallel mass spectrometry method, seven complete sequences of five samples in triplicate over the course of two months were obtained. Since the UV detector was very reliable, and method development was targeted at optimizing MS, ELSD and CAD conditions, multiple sequences of UV data were obtained and are summarized below. Complete and detailed results for all detectors are provided here for the final method and final sequence of samples.

3.1. Vitamin D_3 by UV detection

Table 1 shows the results for the determination of vitamin D_3 in five gelcaps that were each run in triplicate. UV data for the first sample run are shown in Fig. 1A and C for UV at 265 nm and at 210 nm, respectively. Although Table 1 gives values for determinations at both 265 nm and 210 nm, the latter is not recommended for routine analysis, due to decreased specificity. 265 nm is the commonly used detection wavelength for vitamin D_2 and D_3. 210 nm was included in the analysis because it is a more universal detection wavelength, since most species give some absorbance at this wavelength, which increased the likelihood of detecting any potential interfering species. Peaks at 210 nm were smaller relative to the background, as seen in Fig. 1C, which made peak integration more difficult, so results by UV detection at 210 nm are not discussed in detail.

The UV at 265 nm results for individual samples, run in triplicate, were very consistent, as judged by several criteria. For the IS method, the average values ($n = 3$) ranged from 0.2800 to 0.2895 μg/mL, or from 1120 to 1158 IU per capsule (p.c.), and their

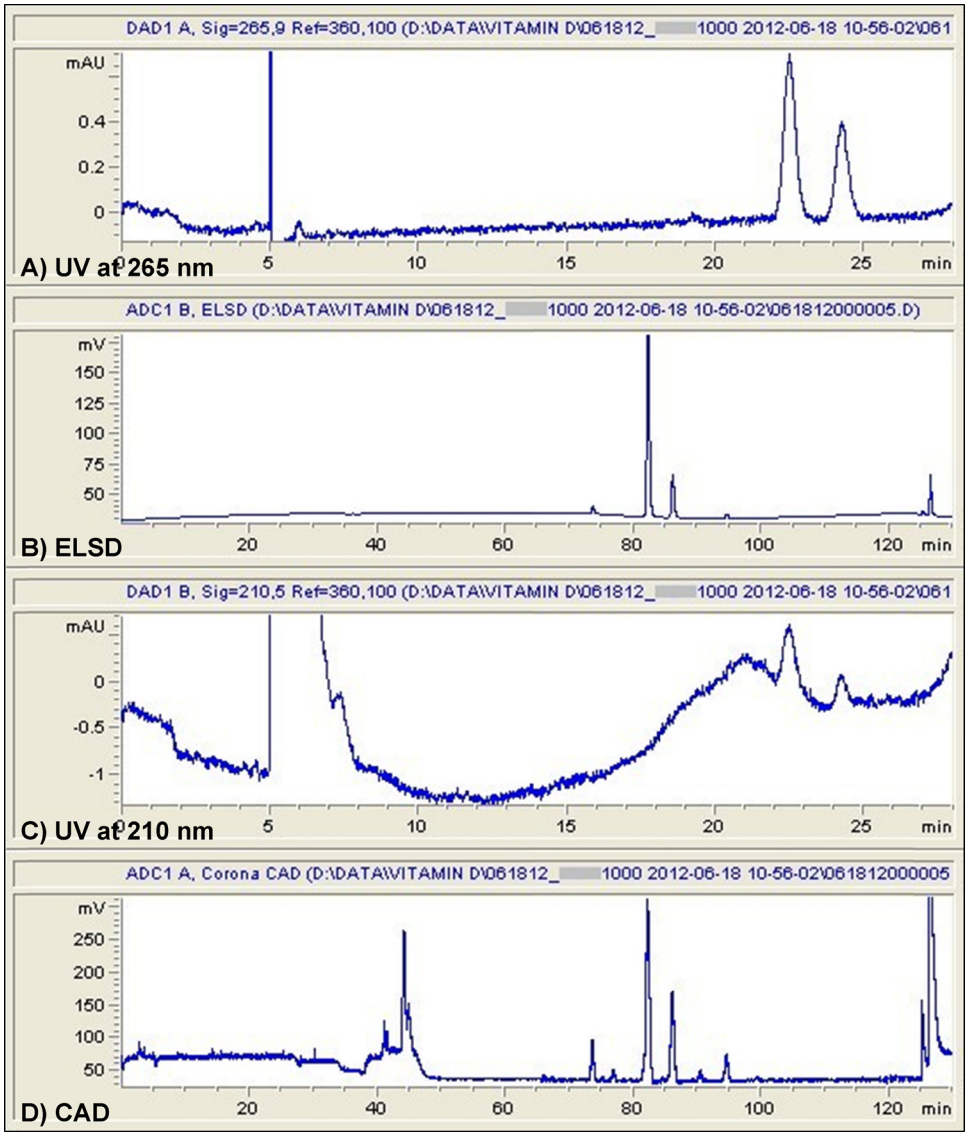

Fig. 1. Ultraviolet (UV) detector, evaporative light scattering detector (ELSD), and corona charged aerosol detector (CAD) chromatograms from dietary supplement gelcap. A) UV at 265 nm; B) ELSD; C) UV at 210 nm; D) Corona CAD. ELSD and CAD signal from Agilent 35900E analog-to-digital converter. Gelcap brand masked for anonymity.

percent relative standard deviations (% RSD) ranged from 0.64% to 3.16%, with the average % RSD being 1.69%. These values typify the run-to-run variability within samples. Across all five samples, the average of the values was 0.2861 ± 0.0044 μg/mL (1.53% RSD), or 1145 ± 17 IU p.c. This uncertainty typifies the sample-to-sample variability by the IS approach. A more rigorous treatment of uncertainty can be provided as the square root of the sum of the squares (SRSS) of the uncertainties in the individual samples, which is ± 0.0126 μg/mL, or 4.42% SRSS.

The ES approach produced results with low uncertainty, but slightly more than IS results, with values from individual samples run in triplicate ranging from 0.2776 to 0.2927 μg/mL, or 1110 to 1171 IU p.c., with % RSD ranging from 0.32% to 2.41%, with the average % RSD of 1.31%. The sample average from all five sample replicates by the ES approach was 0.2870 ± 0.0059 μg/mL (2.07% RSD, 3.49% SRSS), or 1148 ± 24 IU p.c., in good agreement to the IS results. The calibration curve coefficients of determination (R^2) for the IS and ES methods were 0.9996 and 0.9998, respectively.

Perhaps the best measure of the robustness of the UV results obtainable from this method can be demonstrated from the uncertainty in the raw areas of the internal standards in all samples and standards. Since all standards contained 0.500 μg/mL (2000 IU/100 mL) vitamin D_2 IS (calibration standards are used for 60 days at most), and a similar 0.500 μg/mL was added to every sample before dilution to 100 mL, all standards and samples should have the same amount of vitamin D_2 IS. The % RSD in raw integrated areas of the internal standard across all standard runs ($n = 19$) and sample runs ($n = 15$) was 1.35%. This represents the combined uncertainty from pipetting the IS into standards or into samples, injection uncertainty, UV detector response variability, integration variability, and any other factors that affected the raw areas of the IS in the UV at 265 nm chromatograms. This is in good agreement with our previous report that employed the same LC method, which showed 1.15% RSD in raw vitamin D_2 areas [7]. This represents a useful tool for diagnosis of interfering species that elute with vitamin D_2, including pre-vitamin D_3. If the % RSD for the raw areas of the IS across all samples and standards is >∼3.0% using this method, it indicates a potential interferent in the UV at 265 nm. In such cases, the % RSD of the samples will be low and the % RSD of the standards will be low, but when combined the % RSD will be

higher. If pre-vitamin D_3 is present in a substantial amount, it can be estimated by subtracting the average area of the vitamin D_2 IS from the areas of the IS in the samples to give an area attributable to pre-vitamin D_3, which can be estimated on the calibration curve. In the absence of such interference, samples and standards give low % RSDs (1.24% and 1.36%, respectively in this case), and when combined they are close to the overall % RSD (1.35%).

The calibration curve LOD for the ES method was calculated as 0.0174 μg/mL, or 70 IU in a gelcap diluted to 100 mL, while for the IS method the LOD was calculated as 0.0102 μg/mL, or 41 IU per gelcap, which translates to 0.2 ng or 200 pg on column. The calibration curve LOQ by the ES method was calculated as 0.0581 μg/mL, or 232 IU p.c., while for the IS method the LOQ was found to be 0.0339 μg/mL, or 136 IU p.c.

Quantification based on a single RF is similar to the approach used in AOAC method 2002.05. That method used an iRF, based on the ratio of the vitamin D_3/D_2 peaks. It is also possible to compare the raw areas of the sample to the raw area of a standard, in an ES RF approach (eRF). The iRF or eRF can be calculated relative to any of the three calibration standards (low, middle, high), for iRF1, iRF2, and iRF3, or eRF1, eRF2, and eRF3, for IS or ES RF, respectively. For thoroughness and comparison, we calculated all possible approaches. Usually, the iRF or eRF results calculated from the standard closest to the level of vitamin D_3 in the samples gave the results closest to those determined using the IS calibration approach, as would be expected. The iRF results were 1143 ± 17, 1160 ± 17, and 1179 ± 17 for iRF1, iRF2, and iRF3, respectively. The eRF results were 1146 ± 23, 1152 ± 24, and 1154 ± 24 IU for eRF1, eRF2, and eRF3, respectively. Additional detail regarding these approaches applied to other samples was given in the supplementary materials to our previous report [7]. As a matter of principle, iRF1 is preferred, since an IS method is preferred over an ES method, and the labeled sample values were closest to the low calibration standard.

The values from iRF1 given in Table 1 show values for triplicate analyses from 0.2798 to 0.2889 μg/mL, or 1119 to 1156 IU p.c., with uncertainties ranging from 0.61% to 3.04% RSD, and an average % RSD of 1.63%. The average of five samples was 0.2857 ± 0.0042 μg/mL (1.47% RSD, 4.25% SRSS), or 1143 ± 17 IU p.c., in good agreement with the IS and ES results above.

3.2. Vitamin D_3 by APCI-MS

Table 2 shows the results by APCI-MS using SIM, two transitions of SRM (SRM1, which is dehydration, and SRM2 described in Section 2.2.2.1), and by EIC from full-scan runs. Fig. 2 shows the corresponding raw chromatograms and spectra used to obtain these data. Two trends are apparent in Table 2. First, the external standard results have higher standard deviations than IS and iRF results in every case, which is to be expected. An APCI source is inherently noisier than UV detection. Furthermore, in the presence of ACN, a black residue forms over time on the tip of the corona needle. A plot of IS (vitamin D_2) areas and TAG areas over the course of the sequence (not shown) exhibits a distinct, though not linear, loss of signal over time. The calibration curve R^2 values by ES were 0.9312, 0.9230, and 0.9276 for SIM, SRM1, and SRM2, respectively. Thus, the ES method should not be used for reliable quantification of APCI-MS data. The second trend, which was also expected, is the fact that results from EIC from full-scan data gave poorer % RSD than SIM and SRM data. The signal-to-noise ratio (S/N) for EIC was poorer due to the shorter amount of the instrument duty cycle spent at each analyte mass during a full scan (*m/z* 200–2000 in 1.0 s) compared to targeted scans (SIM and SRM) having 0.5 s at each targeted mass. Because of the corona needle residue, by the last replicate of the last sample the vitamin D peaks were not visible in the full-scan TIC, and the peaks in the EIC showed poor S/N. For this reason, full-scans were problematic for vitamin D quantification. The remaining methods for quantification by MS in Table 2 (SIM and SRM, by IS and iRF) had lower % RSD and were effective and reliable for vitamin D analysis.

Table 2
Sample weight normalized amounts of vitamin D_3, in μg/mL, for gelcap contents diluted to 100 mL, determined by atmospheric pressure chemical ionization mass spectrometry (APCI-MS) detection in selected ion monitoring (SIM), selected reaction monitoring (SRM), and full-scan extracted ion chromatogram (EIC) modes. Results by internal standard (IS), external standard (ES), and response factor (iRF) approaches, relative to vitamin D_2 internal standard (0.500 μg/mL = 2000 IU/100 mL).

SIM: *m/z* 367.3, 379.3, 385.3, 397.3		
IS ± SD	ES ± SD	iRF[b] ± SD
0.2774[a] ± 0.0043	0.368 ± 0.019	0.2787 ± 0.0041
0.287 ± 0.019	0.318 ± 0.054	0.288 ± 0.018
0.2879 ± 0.0076	0.252 ± 0.013	0.2901 ± 0.0072
0.281 ± 0.015	0.285 ± 0.013	0.283 ± 0.014
0.291 ± 0.016	0.272 ± 0.022	0.292 ± 0.015
Avg. 0.2849 ± 0.0055	0.299 ± 0.045	0.2863 ± 0.0055
± 0.030[c]	± 0.065	± 0.029
SRM1: *m/z* 385.3 -> 367.3; *m/z* 397.3 -> 379.3		
IS ± SD	ES ± SD	iRF ± SD
0.2901 ± 0.0099	0.358 ± 0.020	0.285 ± 0.010
0.2883 ± 0.0032	0.289 ± 0.018	0.2827 ± 0.0033
0.2763 ± 0.0078	0.248 ± 0.021	0.2695 ± 0.0080
0.3014 ± 0.0029	0.293 ± 0.015	0.2959 ± 0.0030
0.2862 ± 0.0047	0.265 ± 0.016	0.2805 ± 0.0048
Avg. 0.2885 ± 0.0090	0.291 ± 0.042	0.2827 ± 0.0094
± 0.014	± 0.040	± 0.015
SRM2: *m/z* 385.3 -> 259.2; *m/z* 397.3 -> 271.2		
IS ± SD	ES ± SD	iRF ± SD
0.293 ± 0.010	0.344 ± 0.014	0.289 ± 0.010
0.2787 ± 0.0089	0.271 ± 0.020	0.2747 ± 0.0092
0.2934 ± 0.0086	0.233 ± 0.018	0.2889 ± 0.0088
0.300 ± 0.010	0.2997 ± 0.0035	0.297 ± 0.011
0.304 ± 0.011	0.283 ± 0.016	0.301 ± 0.011
Avg. 0.2939 ± 0.0097	0.286 ± 0.040	0.290 ± 0.010
± 0.022	± 0.034	± 0.022
MS: EIC of *m/z* 367.3, 379.3, 385.3, 397.3		
IS ± SD	ES ± SD	iRF ± SD
0.278 ± 0.060	0.37 ± 0.28	0.256 ± 0.032
0.322 ± 0.089	0.58 ± 0.11	0.281 ± 0.048
0.294 ± 0.030	0.263 ± 0.055	0.275 ± 0.016
0.308 ± 0.064	0.267 ± 0.028	0.276 ± 0.035
0.271 ± 0.075	0.22 ± 0.11	0.255 ± 0.040
Avg. 0.294 ± 0.021	0.34 ± 0.15	0.269 ± 0.012
± 0.15	± 0.32	± 0.080

[a] Values and uncertainties are given to 0.0001 μg/mL, or to the second uncertain figure.
[b] Response factor calculated using ratio of 0.25 μg/mL standard to internal standard.
[c] Square root of the sum of the squares of the individual standard deviations.

For the IS approach, SIM gave values from 0.2774 to 0.2911, or 1110 to 1164 IU p.c., with % RSD from 1.56% to 6.57%, which is higher than the % RSD from SRM, but less than the % RSD for the IS method from EIC of full-scan MS. The average value by the IS SIM method was 0.2849 ± 0.0055 μg/mL (1.94% RSD, 10.7% SRSS), or 1140 ± 22 IU p.c., in good agreement with results by UV. The results by iRF for SIM had very similar % RSD, from 1.47% to 6.20%, and a similar and not statistically significantly different average value of 0.2863 ± 0.0055 μg/mL (1.91% RSD, 10.1% SRSS), or 1145 ± 22 IU p.c.

Because ions for SIM were produced in the ion source and did not involve MS/MS, which is not entirely efficient, the average integrated area for the IS was 5.3 times larger by SIM than by SRM1 and 11.8 times larger than by SRM2. But SIM was less specific, since it did not incorporate the specific precursor→ product fragmentation. However, as long as full-scan MS scans are also acquired to prove the absence of interfering species, it is useful to take advantage of the larger signal given by SIM.

Both IS and iRF results by SRM1 gave lower run-to-run % RSD than SIM, ranging from 0.97% to 3.43% for IS and 1.02% to 3.57% for iRF, but the sample-to-sample averages gave lower % RSD

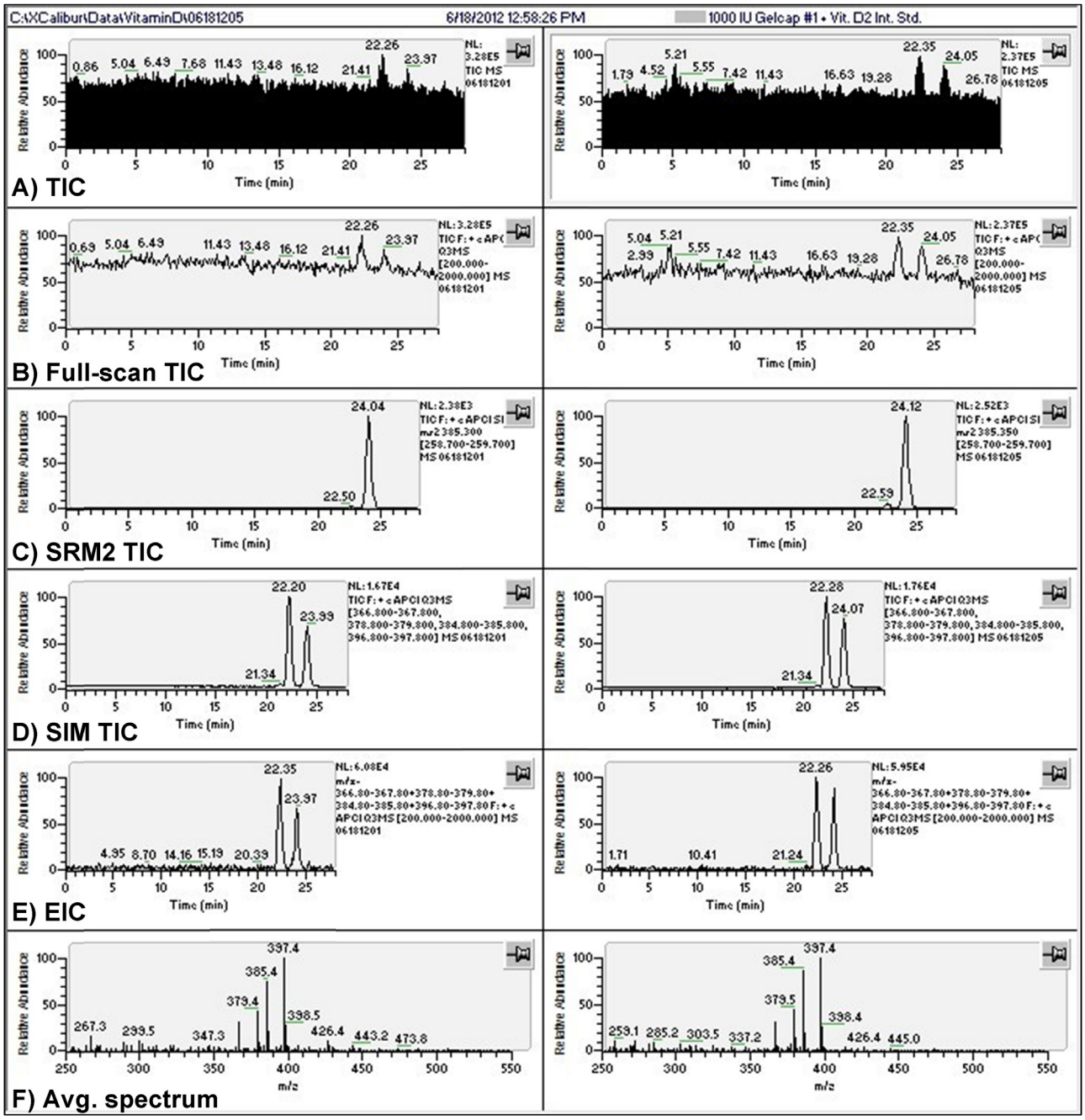

Fig. 2. Atmospheric pressure chemical ionization (APCI) mass spectrometry (MS) data for vitamin D using selected ion monitoring (SIM) mode, selected reaction monitoring (SRM) mode, and extracted ion chromatograms (EIC) from full-scan mode for 0.25 μg/mL (1000 IU/100 mL) vitamin D_3 standard solution (left) and gelcap sample #1 (right), both with 0.5 mg/mL (2000 IU/100 mL) vitamin D_2 internal standard. A) Total ion current chromatogram (TIC) showing alternating scan modes; B) TIC of full scans only; C) TIC of SRM *m/z* 385.3→ 259.2 for vitamin D_3; D) TIC of SIM masses; E) EIC extracted from full-scan mode; F) Average mass spectrum across vitamin D_2 (~22.3 min) and vitamin D_3 (~24 min) peaks. Gelcap brand masked for anonymity.

for SIM than for SRM1 and SRM2. The average values for IS and iRF approaches by SRM1 were 0.2885 ± 0.0090 μg/mL (3.11% RSD, 4.91% SRSS), or 1154 ± 36 IU p.c., and 0.2827 ± 0.0094 (3.34% RSD, 5.13% SRSS), or 1131 ± 38 IU p.c., respectively.

Similarly, IS and iRF results by SRM2 gave lower run-to-run % RSD than SIM, ranging from 2.92% to 3.47% for IS and 3.05 to 3.62% for iRF, but sample-to-sample averages gave a % RSD of 3.32%, which was slightly higher than SRM1, and higher than SIM results. The average of the five sample average values was 0.2939 ± 0.0097 μg/mL (3.32% RSD, 7.37% SRSS), or 1176 ± 39 IU for the IS method, and 0.2901 ± 0.0100 μg/mL (3.44% RSD, 7.70% SRSS), or 1161 ± 40 IU for the iRF approach.

In all comparisons between UV, SIM, SRM1, and SRM2 by IS and iRF approaches, no statistically significant differences were found between five-sample average values. The LOD calculated from the IS method using calibration curves from SIM, SRM1, and SRM2 data were 0.0307 μg/mL (123 IU p.c.), 0.0230 μg/mL (92 IU p.c.), and 0.0263 μg/mL (105 IU p.c.), respectively. The LOQ similarly calculated for the IS method were 0.1023 μg/mL (409 p.c.), 0.0765 μg/mL (306 p.c.), and 0.0875 μg/mL (350 IU p.c.) for the SIM, SRM1, and SRM2 methods, respectively. The calibration curve R^2 was 0.9979

Table 3
Comparison of results between sequences of samples analyzed over two months. Sample weight normalized amounts of vitamin D_3, in μg/mL, for gelcap contents diluted to 100 mL, determined by ultraviolet (UV) detection and by atmospheric pressure chemical ionization mass spectrometry (APCI-MS) detection in selected ion monitoring (SIM) and selected reaction monitoring (SRM) modes. Results by internal standard (IS), external standard (ES), and internal standard response factor (iRF) approaches, relative to vitamin D_2 internal standard (0.500 mg/mL = 2000 IU/100 mL).[a]

	061812	061112	060612	051012	050712	042512	041712	Method Avg.	SD	% RSD
UV-IS	0.2861[b]	0.2842	0.2884	0.2786	0.2793	0.2835	0.2877	0.2840	0.0039	1.36%
UV-ES	0.2870	0.2842	0.2872	0.2823	0.2826	0.2841	0.2879	0.2850	0.0023	0.81%
UV-iRF	0.2857	0.2814	0.2873	0.2784	0.2835	0.2892	0.2933	0.2855	0.0050	1.75%
SIM-IS	0.2849	0.2985	0.2889	0.2952	0.2661	0.2588	0.2655	0.2797	0.0160	5.70%
SIM-iRF	0.2863	0.2963	0.2844	0.2943	0.2567	0.2652	0.2603	0.2777	0.0166	5.96%
SRM1-IS	0.2885	0.2927	0.2857	0.2968	0.2793	0.2803	0.2810	0.2863	0.0067	2.34%
SRM1-iRF	0.2827	0.2884	0.2880	0.3012	0.2775	0.2759	0.2781	0.2845	0.0089	3.12%
SRM2-IS	0.2939	0.2732	0.2906	0.2908	0.2866	0.2763	0.2884	0.2857	0.0078	2.74%
SRM2-iRF	0.2901	0.2904	0.2841	0.2897	0.2809	0.2736	0.2843	0.2847	0.0061	2.15%
Sequence Avg.	0.2872	0.2877	0.2872	0.2897	0.2769	0.2763	0.2807	Meta-Avg.	0.2837[c]	
SD	0.0033	0.0079	0.0021	0.0082	0.0095	0.0096	0.0111	SD	0.0056	
% RSD	1.14%	2.74%	0.73%	2.84%	3.43%	3.47%	3.96%	% RSD	1.96%	
Avg. IU[d]	1149	1151	1149	1159	1108	1105	1123		1135	
SD IU	13	32	8	33	38	38	44		22	

[a] All values represent the averages of five samples run in triplicate, for $n = 15$.
[b] All values given to 0.0001 μg/mL for uniformity, even if more than second uncertain figure required.
[c] Average of values in table ($n = 63$) across all sample dates and all detection methods.
[d] Per capsule average values in International Units, IU, where 1 IU = 0.025 μg.

for the SIM IS method, 0.9980 for SRM1 by IS, and 0.9943 for SRM2 by IS. The ELSD and corona ultra CAD detectors were not sufficiently sensitive to allow quantification of vitamin D_3 at the levels encountered here (~ 1150 IU/100 mL = ~5.75 ng on column from 20 μL injected).

A comparison of results over two months, given in Table 3, provided another means to assess the robustness of the method. Columns represent sequences quantified by different methods, while rows represent quantification methods across all sequences. Excluding the least effective MS methods, the ES method and the

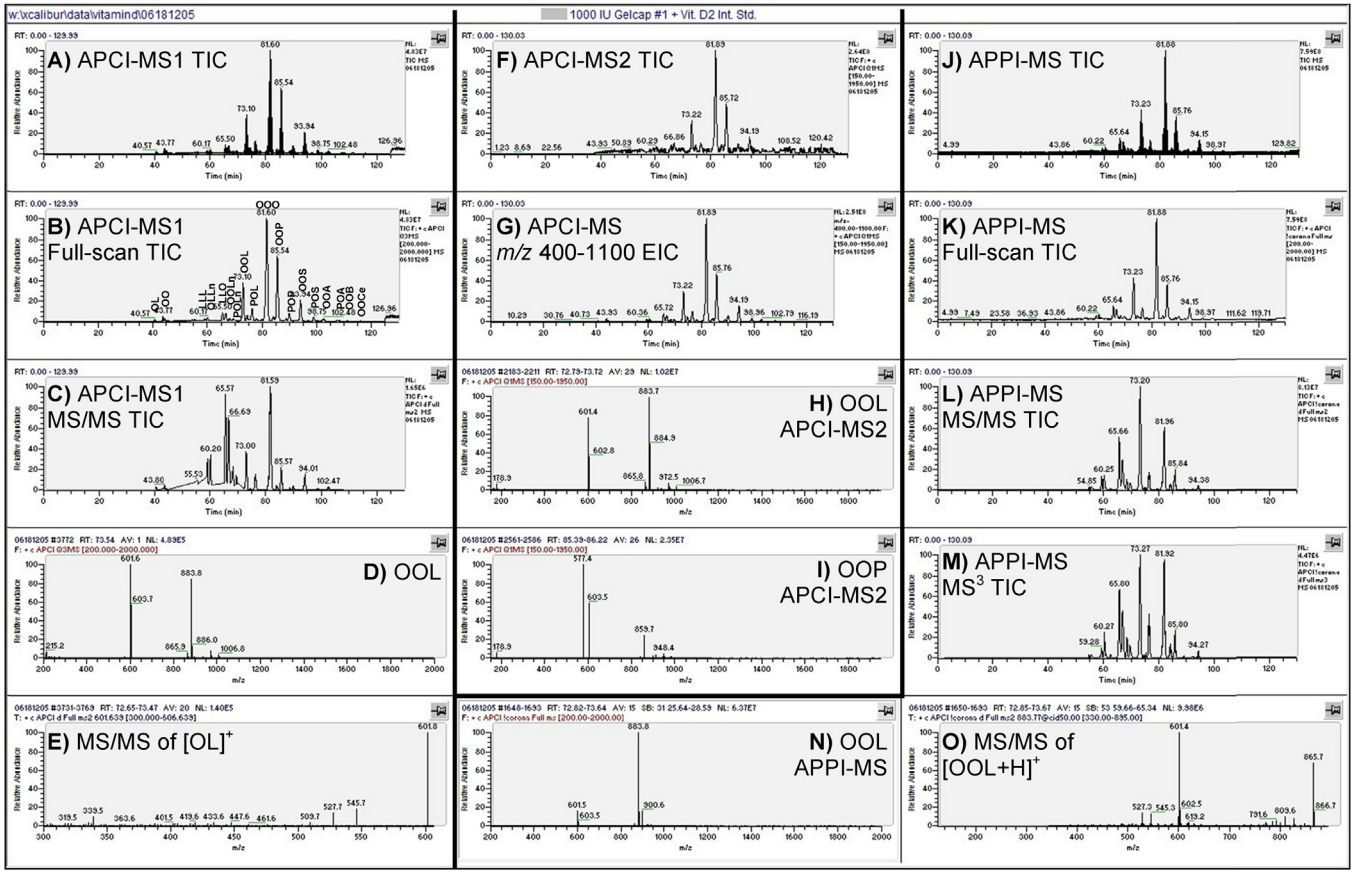

Fig. 3. Two types of atmospheric pressure chemical ionization (APCI) mass spectrometry (MS) plus atmospheric pressure photoionization (APPI) MS chromatograms and mass spectra. **A)** Total ion current chromatogram (TIC) from newest APCI-MS instrument (1); **B)** TIC of APCI-MS1 full scans; **C)** TIC of MS/MS scans from APCI-MS1; **D)** mass spectrum of OOL; **E)** auto-MS/MS mass spectrum of most abundant peak in D); **F)** TIC from older APCI-MS (2); **G)** extracted ion chromatogram of the range *m/z* 400–1100 from APCI-MS2; **H)** mass spectrum of OOL from APCI-MS2; **I)**APCI-MS2 mass spectrum of OOP; **J)** TIC from APPI-MS; **K)** TIC of APPI-MS full scans; **L)** TIC of APPI-MS/MS scans; **M)** TIC of APPI-MS^3 scans; **N)** APPI-MS mass spectrum of OOL; **O)** auto-MS/MS mass spectrum of most abundant peak in N).

Table 4
Triacylglycerol (TAG) compositions of olive oil in dietary supplements determined by atmospheric pressure chemical ionization (APCI) mass spectrometry (MS), atmospheric pressure photoionization (APPI) MS, electrospray ionization (ESI) MS, a corona charged aerosol detector (CAD), and an evaporative light scattering detector (ELSD) simultaneously in parallel. Averages of five samples in triplicate for fifteen runs.

TAG	RT[a]	APCI-MS #1[b] ± SD	APCI-MS #2[c] ± SD	APPI-MS ± SD	ESI-MS	Sat. Adj. ESI-MS[d] ± SD	CAD ± SD	ELSD	±	SD
LnLnLn	47.53	0.01% ± 0.00%	0.00% ± 0.00%	0.02% ± 0.00%	0.02%	0.01% ± 0.01%				
LnLnL	50.71	0.04% ± 0.00%	0.04% ± 0.01%	0.08% ± 0.01%	0.11%	0.05% ± 0.02%				
LLLn	54.52	0.09% ± 0.00%	0.12% ± 0.01%	0.20% ± 0.01%	0.22%	0.11% ± 0.04%				
LnLnO1	55.38	0.13% ± 0.00%	0.17% ± 0.02%	0.30% ± 0.02%	0.38%	0.18% ± 0.05%				
LnLnO2	55.90	0.04% ± 0.00%	0.05% ± 0.01%	0.09% ± 0.01%	0.14%	0.07% ± 0.03%				
LnLnP	57.32	0.01% ± 0.00%	0.01% ± 0.01%	0.03% ± 0.00%	0.05%	0.02% ± 0.01%				
LLL	59.03	0.41% ± 0.01%	0.48% ± 0.05%	0.94% ± 0.03%	1.05%	0.51% ± 0.14%	0.06% ± 0.08%			
OLLn1	60.06	0.59% ± 0.01%	0.71% ± 0.05%	1.28% ± 0.05%	1.62%	0.78% ± 0.11%	0.11% ± 0.12%			
OLLn2	60.70	0.09% ± 0.01%	0.12% ± 0.02%	0.22% ± 0.02%	0.37%	0.18% ± 0.08%				
PoOLn	60.87	0.04% ± 0.00%	0.05% ± 0.01%	0.08% ± 0.01%	0.14%	0.07% ± 0.03%				
PLLn	62.40	0.09% ± 0.00%	0.12% ± 0.01%	0.19% ± 0.01%	0.34%	0.16% ± 0.08%				
PoPLn	63.27	0.01% ± 0.00%	0.01% ± 0.00%	0.02% ± 0.00%	0.05%	0.03% ± 0.01%				
LLO	65.50	1.90% ± 0.03%	2.17% ± 0.12%	3.92% ± 0.08%	3.87%	1.87% ± 0.16%	0.77% ± 0.21%			
PoOL	66.66	0.22% ± 0.01%	0.20% ± 0.02%	0.25% ± 0.01%	0.58%	0.28% ± 0.04%				
OOLn1	66.72	1.91% ± 0.03%	2.20% ± 0.13%	3.79% ± 0.11%	4.42%	2.14% ± 0.21%	0.98% ± 0.26%			
OOLn2	67.43	0.11% ± 0.01%	0.18% ± 0.03%	0.26% ± 0.04%	0.30%	0.14% ± 0.03%				
LLP	68.27	0.49% ± 0.01%	0.61% ± 0.03%	0.95% ± 0.03%	1.55%	0.75% ± 0.18%	0.11% ± 0.10%			
POLn1	69.49	0.50% ± 0.02%	0.67% ± 0.06%	1.08% ± 0.02%	2.06%	1.00% ± 0.17%	0.13% ± 0.12%			
POLn2	71.23	0.01% ± 0.00%	0.00% ± 0.00%	0.00% ± 0.00%	0.02%	0.01% ± 0.00%				
PoPL	69.50	0.09% ± 0.01%	0.10% ± 0.01%	0.08% ± 0.01%	0.21%	0.10% ± 0.02%				
LLG	71.26	0.02% ± 0.00%	0.04% ± 0.01%	0.07% ± 0.00%	0.07%	0.03% ± 0.01%				
PPLn	72.71	0.03% ± 0.00%	0.03% ± 0.01%	0.06% ± 0.01%	0.13%	0.06% ± 0.02%				
OOL	73.13	10.41% ± 0.16%	10.35% ± 0.49%	15.01% ± 0.33%	9.88%	10.40% ± 0.43%	9.01% ± 0.31%	2.49%	0	0.26%
OOPo	74.59	1.32% ± 0.06%	1.41% ± 0.07%	1.14% ± 0.04%	3.71%	1.79% ± 0.24%	0.80% ± 0.20%			
LLS	75.29	0.21% ± 0.01%	0.28% ± 0.03%	0.35% ± 0.02%	0.42%	0.20% ± 0.04%				
POL	76.40	3.46% ± 0.07%	3.56% ± 0.19%	4.04% ± 0.10%	6.71%	3.25% ± 0.22%	2.69% ± 0.39%	0.24%	0	0.11%
SOLn	76.50	0.17% ± 0.00%	0.19% ± 0.02%	0.37% ± 0.01%	0.47%	0.23% ± 0.06%				
OOM	78.09	0.21% ± 0.01%	0.25% ± 0.01%	0.20% ± 0.01%	0.66%	0.32% ± 0.10%	0.10% ± 0.07%			
POPo	78.10	0.38% ± 0.03%	0.49% ± 0.01%	0.27% ± 0.01%	1.21%	0.59% ± 0.19%	0.18% ± 0.12%			
OLG	79.53	0.13% ± 0.01%	0.17% ± 0.01%	0.27% ± 0.01%	0.37%	0.18% ± 0.08%				
PPL	80.05	0.20% ± 0.02%	0.26% ± 0.01%	0.11% ± 0.01%	1.24%	0.60% ± 0.16%	0.06% ± 0.08%			
OOO	81.82	41.55% ± 1.20%	40.40% ± 1.51%	40.38% ± 0.50%	17.42%	41.00% ± 1.10%	49.00% ± 3.32%	78.17%	0	0.71%
SLO	84.22	1.18% ± 0.03%	1.24% ± 0.13%	1.60% ± 0.05%	2.84%	1.38% ± 0.20%	0.63% ± 0.15%			
OOP	85.75	20.90% ± 0.33%	19.91% ± 0.49%	13.42% ± 0.26%	14.41%	20.40% ± 0.73%	23.49% ± 0.61%	17.21%	0	0.37%
SLP	88.40	0.13% ± 0.01%	0.17% 0 0.01%	0.09% ± 0.01%	0.71%	0.34% ± 0.11%				
OOG	89.03	0.58% ± 0.03%	0.61% ± 0.05%	0.63% ± 0.03%	1.20%	0.58% ± 0.11%	0.18% ± 0.14%			
POP	90.14	2.23% ± 0.11%	2.52% ± 0.07%	0.98% ± 0.04%	5.57%	2.70% ± 0.35%	2.54% ± 0.36%	0.17%	0	0.08%
LOA	92.34	0.12% ± 0.01%	0.15% ± 0.02%	0.22% ± 0.01%	0.36%	0.17% ± 0.06%				
POG	93.51	0.14% ± 0.02%	0.20% ± 0.02%	0.16% ± 0.02%	0.58%	0.28% ± 0.12%	0.03% ± 0.04%			
OOS	94.30	7.09% ± 0.12%	6.38% ± 0.29%	4.64% ± 0.12%	7.33%	3.55% ± 0.35%	7.28% ± 0.58%	1.71%	0	0.16%
PPP	96.87	0.01% ± 0.00%	0.01% ± 0.00%	0.00% ± 0.00%	0.06%	0.03% ± 0.01%				
PLA	96.96	0.02% ± 0.00%	0.03% ± 0.01%	0.03% ± 0.00%	0.08%	0.04% ± 0.02%				
SSL	97.09	0.03% ± 0.00%	0.05% ± 0.01%	0.03% ± 0.01%	0.13%	0.06% ± 0.03%				
POS	99.10	1.16% ± 0.07%	1.32% ± 0.07%	0.58% ± 0.02%	3.20%	1.55% ± 0.20%	1.12% ± 0.33%			
OLB	100.63	0.04% ± 0.00%	0.05% ± 0.01%	0.08% ± 0.00%	0.12%	0.06% ± 0.02%				
SOG	102.08	0.02% ± 0.00%	0.04% ± 0.01%	0.03% ± 0.01%	0.10%	0.05% ± 0.02%				
OOA	102.91	0.71% ± 0.04%	0.78% ± 0.05%	0.63% ± 0.02%	1.45%	0.70% ± 0.11%	0.53% ± 0.25%			
PBL	105.40	0.00% ± 0.00%	0.01% ± 0.00%	0.01% ± 0.00%	0.02%	0.01% ± 0.00%				
SLA	105.86	0.00% ± 0.00%	0.01% ± 0.00%	0.01% ± 0.00%	0.02%	0.01% ± 0.00%				
PPS	106.92	0.00% ± 0.00%	0.00% ± 0.00%	0.00% ± 0.00%	0.02%	0.01% ± 0.00%				
OO-21	107.19	0.02% ± 0.00%	0.03% ± 0.00%	0.03% ± 0.00%	0.05%	0.02% ± 0.01%				
POA	108.09	0.16% ± 0.02%	0.21% ± 0.02%	0.14% ± 0.00%	0.44%	0.21% ± 0.07%	0.07% ± 0.06%			
SSO	108.26	0.24% ± 0.03%	0.32% ± 0.03%	0.17% ± 0.01%	0.66%	0.32% ± 0.10%	0.10% ± 0.09%			
OLLg	108.89	0.01% ± 0.00%	0.02% ± 0.01%	0.04% ± 0.00%	0.03%	0.01% ± 0.01%				

Table 4 (*Continued*)

TAG	RT[a]	APCI-MS #1[b] ± SD	APCI-MS #2[c] ± SD	APPI-MS ± SD	ESI-MS	Sat. Adj. ESI-MS[d] ± SD	CAD ± SD	ELSD	±	SD
OOB	111.59	0.16% ± 0.02%	0.20% ± 0.02%	0.18% ± 0.01%	0.41%	0.20% ± 0.07%	0.04% ± 0.07%			
PLLg	113.26	0.00% ± 0.00%	0.00% ± 0.00%	0.00% ± 0.00%	0.01%	0.01% ± 0.00%				
SLB	113.67	0.00% ± 0.00%	0.00% ± 0.00%	0.00% ± 0.00%	0.01%	0.00% ± 0.00%				
OO-23	114.29	0.02% ± 0.00%	0.04% ± 0.00%	0.04% ± 0.00%	0.07%	0.04% ± 0.02%				
POB	114.83	0.03% ± 0.00%	0.05% ± 0.01%	0.03% ± 0.00%	0.07%	0.03% ± 0.01%				
SOA	115.07	0.03% ± 0.00%	0.04% ± 0.01%	0.03% ± 0.00%	0.06%	0.03% ± 0.01%				
OOLg	116.03	0.06% ± 0.01%	0.07% ± 0.01%	0.08% ± 0.00%	0.13%	0.06% ± 0.06%				
OO-25	117.33	0.01% ± 0.00%	0.02% ± 0.00%	0.02% ± 0.00%	0.02%	0.01% ± 0.01%				
POLg	117.72	0.01% ± 0.00%	0.02% ± 0.00%	0.02% ± 0.00%	0.03%	0.01% ± 0.01%				
SOB	117.95	0.00% ± 0.00%	0.01% ± 0.00%	0.01% ± 0.00%	0.01%	0.01% ± 0.00%				
OOCe	118.33	0.01% ± 0.00%	0.01% ± 0.00%	0.01% ± 0.00%	0.01%	0.00% ± 0.01%				
SOLg	119.47	0.00% ± 0.00%	0.01% ± 0.00%	0.00% ± 0.00%	0.00%	0.00% ± 0.00%				
Sum	100.00%	100.00%	100.00%	100.00%	100.00%	100.00%	100.00%			
DAG/TAG[e]	1.65% ± 0.10%	1.67% ± 0.09%	0.49% ± 0.03%	3.55%	1.72% ± 0.24%	21.97% ± 7.90%	0.08% ± 0.07%			

[a] Average retention times ($n = 15$) from TSQ Vantage EMR used for vitamin D_3 quantification.
[b] APCI-MS on high-sensitivity mass spectrometer, TSQ Vantage EMR.
[c] APCI-MS on low-sensitivity mass spectrometer, TSQ 7000.
[d] ESI-MS data recalculated setting OOL to 10.4%,OOO to 41.0%, and OOP to 20.4% assuming charge saturation of these three peaks.
[e] Ratio of total area for diacylglycerols (DAG) versus TAG.

EIC from full scans, and excluding UV methods by eRF2, eRF3, iRF2 and iRF3, the average values obtained from the remaining nine approaches, which represent the best options for analysis, was 0.2872 ± 0.0033 μg/mL (1.14% RSD), or 1149 ± 13 IU p.c., for the sequence of samples described in detail herein (061812). Two sequences of samples, labeled 050712 and 042512 were statistically significantly different from the final sequence, 061812, giving values of 1108 ± 38 and 1105 ± 38 IU p.c., respectively, which represent differences of 3.56% and 3.80%, respectively. These are rather low percentage differences, and are statistically significant mainly due to the low % RSD between quantification approaches. The trends described above are further borne out in Table 3. All results by MS gave higher %RSD than all UV results (compare row averages), and the SIM MS results showed higher % RSD than SRM results. The difference between the highest method average (SRM1 IS) and lowest method average (SIM RF) values over time was not statistically significant. Across all nine detection methods and quantification approaches applied to seven sequences over the course of two months, the meta-average was 0.2837 ± 0.0056 (1.96% RSD), or 1135 ± 22 IU p.c.

3.3. TAG and FA compositions by APCI-MS

Fig. 3 shows chromatograms and mass spectra obtained on the two APCI-MS instruments and the APPI-MS instrument for easy direct comparison. Ionization sources from different manufacturers behave differently, and even different versions of sources from the same manufacturer (e.g. collinear versus orthogonal) show differences. Fragment ratios can also be affected by tuning and optimization parameters. Differences can be seen, for instance, between the spectra of OOL in Fig. 3D and H, from the TSQ Vantage and older TSQ7000, respectively, which employ orthogonal and collinear source configurations, respectively. The ratio of the $[M+H]^+$ peak to the $[DAG]^+$ is larger in Fig. 3H than in Fig. 3D. Nevertheless, both spectra show good S/N and easily allow identification of the molecular species as OOL based on the protonated molecules, $[M+H]^+$, at *m/z* 883.7 ±0.1 and the diacylglycerol-like fragment ions, $[DAG]^+$, *m/z* 603.5 ± 0.1 for $[OO]^+$ and *m/z* 601.5 ± 0.1 for $[OL]^+$.

TAG were quantified using $[M+H]^+$ and $[DAG]^+$ fragment masses, with all ions for each TAG grouped into a single EIC. We further improved the method by increasing the magnitude of the extracted signal by approximately 30–50% by including the $1 \times {}^{13}C$ isotope for each peak, since this caused no overlap between molecular species, as mentioned in Section 2.2.4. above. The validity of this approach is verified in Fig. 4, which shows peaks present at the level of 0.01% in Table 4. Fig. 4A and B show the same peak profile, but the manually integrated area of the peak (labeled "MA" above peaks) in Fig. 4B is 36% larger because it includes the $1 \times {}^{13}C$ isotopic peaks of the $[DAG]^+$ and $[M+H]^+$ peaks shown in the mass spectrum of OO-25 (C18:1,C18:1,C25:0) shown in Fig. 4C. Similarly, Fig. 4D and E show the EIC and mass spectrum of OOCe (C18:1,C18:1,C26:0), with the EIC including the $1 \times {}^{13}C$ isotopic variant of the main peaks in the mass spectrum.

Peaks in the EIC of grouped ions gave better S/N versus peaks in the TIC chromatograms, since only a few ions out of the scan range *m/z* 200–2000 were extracted, with the remainder constituting background noise for each TAG. This is still not as effective as extracting each individual mass for each $[DAG]^+$ and $[M+H]^+$ separately, which would require two times as many separate peaks to be integrated for AAA TAG (mono-FA, or Type I TAG), three times as many peaks for AAB TAG (two-FA, or Type II TAG), and four times as many peaks to be integrated for ABC TAG (three-FA, or Type III TAG) compared to grouping them in a single EIC. Given that more than 100 DAG and TAG peaks were integrated for each of 15 sample runs on each of four instruments (~$100 \times 15 \times 4 = 6000$

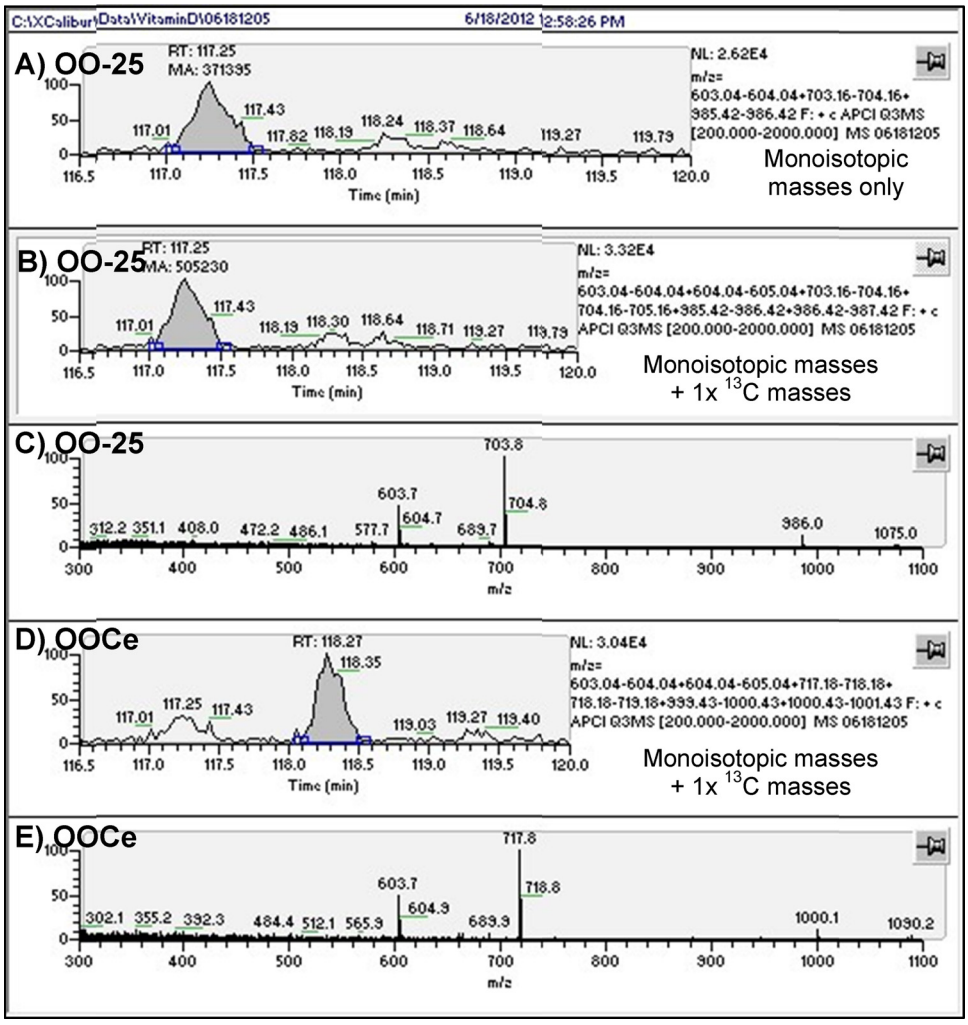

Fig. 4. Extracted ion chromatograms (EIC) and mass spectra of triacylglycerols (TAG) present at a level of 0.01% demonstrating the inclusion of $1 \times {}^{13}C$ isotopic peaks in integrated areas. **A)** C18:1,C18:1,C25:0 (OO-25) extracted calculated masses 603.54,703.66, and 985.92, representing $[OO]^+$, $[O\text{-}25]^+$, and $[OO\text{-}25 + H]^+$, respectively; **B)** OO-25 extracted calculated masses 603.54, 604.54, 703.66, 704.66, 985.92, and 986.92, representing $[OO]^+$, $[O\text{-}25]^+$, and $[OO\text{-}25 + H]^+$, and their $1 \times {}^{13}C$ isotopic variants, respectively; **C)** Average mass spectrum across OO-25 peak; **D)** C18:1,C18:1,C26:0 (OOCe) extracted calculated masses 603.54, 604.54, 717.68, 718.68, 999.93, and 1000.93 representing $[OO]^+$, $[OCe]^+$, and $[OOCe]^+$, and their $1 \times {}^{13}C$ isotopic variants, respectively. **E)** Average mass spectrum across OOCe peak.

peaks integrated), this was a reasonable compromise. Nevertheless, it had the disadvantage that integration of grouped EIC peaks did not allow calculation of critical ratios that allow regioisomer compositions and other structural characteristics to be determined, as well as reconstruction of the $[DAG]^+$ and $[M + H]^+$ peaks in all mass spectra, as previously demonstrated [20]. For this reason, regioisomers are not discussed here, and TAG labels in the tables do not identify regiospecificity. Furthermore, the individual EIC approach allows more molecular species present at low levels to be identified. Nevertheless, the TAG identified in Table 4 comprise all of the TAG visible in the TIC.

Several Ln-containing TAG (specifically LnLnO, OLLn, OOLn, and POLn) were split into two isomer peaks, which were quantified separately. The isomers had identical masses by definition, and thus could not be differentiated by mass. The mass spectra were not sufficiently different to identify them as different regioisomers or to specify whether they were double bond isomers.

The samples used for this report were ~100 mg gelcaps diluted to 100 mL, for ~1 mg/mL solutions. This concentration did not create problems for the very sensitive APCI-MS tandem sector quadrupole instrument (TSQ Vantage EMR), but sample weights much above this did cause shifting mass assignments by as much as ~ m/z 0.5 and errors in the isotopic abundance ratios. Some brands of gelcaps (survey of brands to be reported elsewhere) were larger (~500 mg) and caused difficulties for the most sensitive instrument. Therefore, for a more universally applicable method, APCI-MS data were also acquired on an older, less sensitive instrument similar to what we have previously used for TAG analysis in more concentrated samples. For the smaller gelcaps described here, use of both APCI-MS instruments provided independent confirmation and verification of APCI-MS results.

The APCI-MS percentages in Table 4 are pretty close to each other, especially for TAG present at levels above 1%. For instance, LLO = 1.90% and 2.17%, OOLn1 = 1.91% and 2.20%, OOL = 10.41% and 10.35% for APCI-MS1 and APCI-MS2, respectively. Normally we could say that these two instruments provided good agreement to each other. However, since the % RSD in Table 4 are small, and these data were obtained from the same samples at the same time, in parallel, the differences between these two instruments are real, and arise from differences in ionization sources, ion path differences (orthogonal vs. collinear inlets, etc.), tuning, and a combination of all other instrumental factors. Other factors, such as run-to-run differences in peak area integration, etc., are incorporated into the % RSD values. In most cases, the values by APCI-MS2 are slightly higher than those by APCI-MS1, except for the four primary TAG in olive oil, OOL, OOO, OOP, and OOS.

Table 5
Fatty acid (FA) compositions determined by gas chromatography (GC) with flame ionization detection (FID) and calculated from the diacylglycerol and triacylglycerol compositions of olive oil in dietary supplements determined by atmospheric pressure chemical ionization (APCI) mass spectrometry (MS), atmospheric pressure photoionization (APPI) MS, electrospray ionization (ESI) MS, a corona charged aerosol detector (CAD), and an evaporative light scattering detector (ELSD) simultaneously in parallel.

FA	GC-FID[a] ± SD	APCI-MS #1[b] ± SD	APCI-MS #2[c] ± SD	APPI-MS ± SD	ESI-MS	Sat. Adj. ESI-MS[d] ± SD	CAD ± SD	ELSD ± SD
M	0.02% ± 0.00%	0.07% ± 0.00%	0.08% ± 0.00%	0.07% ± 0.00%	0.22%	0.11% ± 0.03%	0.03% ± 0.02%	
Po	0.75% ± 0.01%	0.68% ± 0.04%	0.76% ± 0.03%	0.62% ± 0.02%	1.93%	0.95% ± 0.13%	0.33% ± 0.11%	
P	11.03% ± 0.07%	10.79% ± 0.27%	11.00% ± 0.24%	7.81% ± 0.11%	15.10%	11.82% ± 0.36%	11.00% ± 0.50%	5.93% ± 0.12%
Ln	1.11% ± 0.03%	1.36% ± 0.02%	1.65% ± 0.10%	2.87% ± 0.05%	3.77%	1.85% ± 0.11%	0.41% ± 0.16%	
L	6.76% ± 0.20%	7.87% ± 0.14%	8.44% ± 0.31%	12.48% ± 0.11%	13.58%	8.50% ± 0.24%	4.81% ± 0.57%	0.91% ± 0.11%
O	76.19% ± 0.29%	74.96% ± 0.59%	73.67% ± 0.66%	72.53% ± 0.20%	58.01%	73.16% ± 0.50%	80.06% ± 1.87%	92.59% ± 0.26%
S	3.24% ± 0.02%	3.50% ± 0.09%	3.47% ± 0.12%	2.71% ± 0.04%	5.53%	2.71% ± 0.17%	3.08% ± 0.40%	0.57% ± 0.05%
A	0.38% ± 0.01%	0.35% ± 0.03%	0.41% ± 0.02%	0.35% ± 0.01%	0.79%	0.38% ± 0.05%	0.20% ± 0.10%	
G	0.30% ± 0.00%	0.30% ± 0.02%	0.35% ± 0.02%	0.39% ± 0.01%	0.75%	0.37% ± 0.08%	0.07% ± 0.05%	
21	0.02% ± 0.00%	0.01% ± 0.00%	0.01% ± 0.00%	0.01% ± 0.00%	0.02%	0.01% ± 0.00%		
B	0.11% ± 0.00%	0.08% ± 0.01%	0.11% ± 0.01%	0.10% ± 0.00%	0.20%	0.10% ± 0.02%	0.01% ± 0.02%	
23	0.02% ± 0.00%	0.01% ± 0.00%	0.01% ± 0.00%	0.01% ± 0.00%	0.02%	0.01% ± 0.01%		
Lg	0.05% ± 0.00%	0.03% ± 0.00%	0.04% ± 0.00%	0.05% ± 0.00%	0.07%	0.03% ± 0.02%		
25	0.01% ± 0.00%	0.003%[e] ± 0.000%	0.01% ± 0.00%	0.01% ± 0.00%	0.01%	0.00% ± 0.00%		
Ce	0.01% ± 0.00%	0.002%[e] ± 0.000%	0.00% ± 0.00%	0.00% ± 0.00%	0.00%	0.00% ± 0.00%		
Sum	100.00%	100.00%	100.00%	100.00%	100.00%	100.00%	100.00%	100.00%

[a] Average of fifteen determinations obtained using AOCS method Ce 1b-89 converted to mole percentage composition.
[b] APCI-MS on high-sensitivity mass spectrometer, TSQ Vantage EMR.
[c] APCI-MS on low-sensitivity mass spectrometer, TSQ 7000.
[d] ESI-MS data recalculated setting OOL to 10.4%,OOO to 41.0%, and OOP to 20.4% assuming charge saturation of these three peaks.
[e] Value to 0.001% for demonstration purposes.

So, even though the values are all close, the question arises, which composition is closest to the "true" composition? The best way to determine this is to perform calibration of every TAG present using authentic standards present near the level encountered in the sample, similar to the method used for vitamin D, above. Of course this is not practical or possible (standards are available for only a relatively few TAG), and is never done. A compromise might be to calibrate a few species, and assume similar response for others, but that does not reduce uncertainty, since response and APCI-MS fragment ratios depend on differences in the degree of unsaturation, different chain lengths [21], and even the positions of double bonds on the fatty acyl chain [22]. The fragment ratios also depend on the regioisomer composition [23–25], but this is reported to have a minimal impact on response [21]. Theoretically, if all TAG responded equally (which they do not) the TAG composition should yield a fatty acid composition calculated from the TAG that matches the FA composition determined by a second, independent, technique. The method of Byrdwell et al. [26,27] compared the FA composition determined by calibrated GC-FID to the FA composition calculated from the TAG composition to calculate RF for each FA, which are then used to calculate RF for TAG. That approach is applied here.

Table 5 shows the FA composition calculated from APCI-MS1 and APCI-MS2, as well as by calibrated GC-FID. Of course, the weight percentage determined by GC-FID needed to be converted to a mole percentage composition for valid comparison to the FA composition calculated from LC-MS. For demonstration purposes, the percentages of C25:0 and C26:0 (Ce), which rounded to 0.00% are shown to one extra significant figure to show the percentages in the FA composition that gave rise to the peaks in Fig. 4.

While the agreement between GC-FID and APCI-MS in Table 5 is already fairly good, agreement was improved by application of the method of Byrdwell et al. [27], especially for the ESI-MS and APPI-MS results, discussed below. A response factor (Supplemental Table 1) was calculated for each FA by taking the ratio of the FA determined from GC-FID to that determined from DAG plus TAG by APCI-MS. Then, the FA RF for each FA in DAG and TAG were multiplied together to yield a DAG or TAG RF. Each DAG and TAG RF was multiplied times the DAG and TAG composition for each run and then renormalized to 100%, as presented in Table 6. RF-normalized results could be accomplished using just the averages in Table 4, but multiplying RF times the average composition would not provide values for run-to-run standard deviations (SD) or a DAG/TAG ratio, so RF were multiplied times the raw areas that gave the individual DAG and TAG compositions, and new SD and DAG/TAG were calculated. Finally, a new FA composition was calculated from the RF-adjusted DAG and TAG compositions. The FA composition from the RF-adjusted TAG composition in Table 6 is given in Table 7. The RF were normalized to the smallest RF for those components present at ≥0.3% (i.e., Po, P, Ln, L, O, S, G, A). While normalizing the RF is not mathematically necessary to calculate TAG RF, it allows easier comparison of the RF from FA to identify trends.

One trend that was clear was that the polyunsaturated TAG linolenic acid (18:3) gave higher response by all API-MS techniques, for those components present at ≥0.3%, and thus had a FA RF of 1.000000 for all three API-MS methods on all four instruments (Supplemental Table 1). The second smallest RF came from linoleic acid (18:2) for APCI-MS and APPI-MS. This indicated that these API-MS techniques favored polyunsaturated TAG. This can be seen upon re-examination of Table 5, which shows that the Ln and L peaks show the greatest relative percentage difference to the GC-FID results. This effect of unsaturation on TAG quantification is expected, given the dependence of the abundances of the $[M+H]^+$ and $[DAG]^+$ on the degree of unsaturation, as reported ever since the initial report of LC-APCI-MS of TAG [28], and seen here by comparing Fig. 3H (OOL) to Fig. 3I (OOP). It is also noteworthy that the early-eluting polyunsaturated FA-containing TAG also gave better response to APCI-MS/MS, as seen from the larger peaks in Fig. 3C, compared to the full-scan TIC in Fig. 3B. This contrasts to our earlier report [27], which used a different instrument, but a similar APCI source from the same manufacturer. That report gave the lowest RF for palmitic acid, and highest RF for linolenic acid. This again highlights the differences in response that arise from different sources, tuning parameters, and other factors, which again emphasizes the need to compare LC-MS results to GC-FID results for every sample, since there are no universally applicable RF.

Table 7 shows excellent agreement between the GC-FID FA mole percentage composition and the FA composition from the RF-adjusted TAG composition. Since the FA composition by GC-FID is calculated relative to a calibrated standards mixture of known composition, it serves as an objective measure of the FA composition independent of any factors that affect the LC-MS composition. Thus,

Table 6
Response factor adjusted triacylglycerol (TAG) compositions of olive oil in dietary supplements determined by APCI-MS, APPI-MS, and ESI-MS. Averages of five samples in triplicate, adjusted using response factors calculated from fatty acid composition determined by gas chromatography with flame ionization detection.

TAG	APCI-MS #1[a] ± SD	APCI-MS #2[b] ± SD	APPI-MS ± SD	ESI-MS ± SD	Sat. Adj. ESI-MS[c] ± SD
LnLnLn	0.00% ± 0.00%	0.00% ± 0.00%	0.00% ± 0.00%	0.00% ± 0.00%	0.00% ± 0.00%
LnLnL	0.02% ± 0.00%	0.02% ± 0.00%	0.01% ± 0.00%	0.00% ± 0.00%	0.01% ± 0.01%
LLLn	0.05% ± 0.00%	0.05% ± 0.01%	0.02% ± 0.00%	0.02% ± 0.01%	0.04% ± 0.02%
LnLnO1	0.09% ± 0.00%	0.08% ± 0.01%	0.05% ± 0.00%	0.04% ± 0.01%	0.07% ± 0.02%
LnLnO2	0.03% ± 0.00%	0.02% ± 0.00%	0.01% ± 0.00%	0.02% ± 0.01%	0.03% ± 0.01%
LnLnP	0.01% ± 0.00%	0.01% ± 0.00%	0.01% ± 0.00%	0.00% ± 0.00%	0.01% ± 0.00%
LLL	0.26% ± 0.00%	0.25% ± 0.02%	0.15% ± 0.00%	0.13% ± 0.04%	0.26% ± 0.07%
OLLn1	0.42% ± 0.01%	0.40% ± 0.03%	0.28% ± 0.01%	0.32% ± 0.05%	0.39% ± 0.06%
OLLn2	0.07% ± 0.01%	0.07% ± 0.01%	0.05% ± 0.00%	0.07% ± 0.03%	0.09% ± 0.04%
PoOLn	0.04% ± 0.00%	0.04% ± 0.01%	0.04% ± 0.00%	0.02% ± 0.01%	0.03% ± 0.01%
PLLn	0.06% ± 0.00%	0.06% ± 0.01%	0.06% ± 0.00%	0.04% ± 0.02%	0.07% ± 0.03%
PoPLn	0.01% ± 0.00%	0.01% ± 0.00%	0.01% ± 0.00%	0.00% ± 0.00%	0.01% ± 0.01%
LLO	1.43% ± 0.02%	1.44% ± 0.08%	1.20% ± 0.02%	1.30% ± 0.11%	1.23% ± 0.11%
PoOL	0.21% ± 0.01%	0.17% ± 0.02%	0.17% ± 0.01%	0.15% ± 0.02%	0.18% ± 0.03%
OOLn1	1.61% ± 0.03%	1.58% ± 0.10%	1.61% ± 0.05%	2.33% ± 0.22%	1.40% ± 0.13%
OOLn2	0.09% ± 0.01%	0.13% ± 0.02%	0.11% ± 0.02%	0.16% ± 0.03%	0.09% ± 0.02%
LLP	0.37% ± 0.01%	0.39% ± 0.02%	0.39% ± 0.01%	0.29% ± 0.07%	0.44% ± 0.10%
POLn1	0.42% ± 0.01%	0.47% ± 0.04%	0.62% ± 0.01%	0.60% ± 0.10%	0.58% ± 0.10%
POLn2	0.00% ± 0.00%	0.00% ± 0.00%	0.00% ± 0.00%	0.01% ± 0.00%	0.01% ± 0.00%
PoPL	0.08% ± 0.01%	0.08% ± 0.01%	0.08% ± 0.01%	0.03% ± 0.01%	0.06% ± 0.01%
LLG	0.02% ± 0.00%	0.02% ± 0.00%	0.02% ± 0.00%	0.01% ± 0.00%	0.02% ± 0.01%
PPLn	0.02% ± 0.00%	0.02% ± 0.00%	0.05% ± 0.01%	0.02% ± 0.01%	0.03% ± 0.01%
OOL	9.24% ± 0.14%	8.86% ± 0.44%	8.90% ± 0.21%	8.78% ± 0.37%	8.96% ± 0.38%
OOPo	1.51% ± 0.07%	1.50% ± 0.08%	1.53% ± 0.05%	2.58% ± 0.34%	1.55% ± 0.21%
LLS	0.15% ± 0.01%	0.17% ± 0.02%	0.12% ± 0.01%	0.06% ± 0.01%	0.15% ± 0.03%
POL	3.09% ± 0.06%	2.95% ± 0.17%	3.22% ± 0.08%	3.32% ± 0.23%	2.51% ± 0.18%
SOLn	0.13% ± 0.00%	0.13% ± 0.01%	0.18% ± 0.01%	0.11% ± 0.03%	0.17% ± 0.04%
OOM	0.07% ± 0.00%	0.07% ± 0.00%	0.07% ± 0.00%	0.12% ± 0.04%	0.07% ± 0.02%
POPo	0.44% ± 0.04%	0.50% ± 0.01%	0.48% ± 0.02%	0.47% ± 0.15%	0.45% ± 0.15%
OLG	0.12% ± 0.01%	0.13% ± 0.01%	0.12% ± 0.01%	0.10% ± 0.05%	0.12% ± 0.06%
PPL	0.18% ± 0.02%	0.21% ± 0.01%	0.11% ± 0.01%	0.34% ± 0.09%	0.41% ± 0.11%
OOO	43.59% ± 1.23%	44.60% ± 1.52%	46.44% ± 0.56%	40.81% ± 1.12%	46.23% ± 1.15%
SLO	0.95% ± 0.03%	0.96% ± 0.10%	1.08% ± 0.04%	1.13% ± 0.17%	1.36% ± 0.20%
OOP	22.06% ± 0.36%	21.31% ± 0.56%	20.75% ± 0.38%	18.79% ± 0.73%	20.62% ± 0.75%
SLP	0.10% ± 0.01%	0.13% ± 0.01%	0.08% ± 0.01%	0.16% ± 0.05%	0.31% ± 0.09%
OOG	0.61% ± 0.03%	0.56% ± 0.05%	0.54% ± 0.03%	0.86% ± 0.17%	0.52% ± 0.10%
POP	2.36% ± 0.12%	2.62% ± 0.07%	2.03% ± 0.07%	4.04% ± 0.54%	2.44% ± 0.32%
LOA	0.12% ± 0.01%	0.12% ± 0.01%	0.13% ± 0.01%	0.12% ± 0.04%	0.14% ± 0.05%
POG	0.15% ± 0.02%	0.18% ± 0.02%	0.19% ± 0.02%	0.23% ± 0.10%	0.23% ± 0.10%
OOS	6.77% ± 0.12%	6.37% ± 0.30%	6.07% ± 0.15%	7.67% ± 0.74%	4.59% ± 0.46%
PPP	0.01% ± 0.00%	0.01% ± 0.00%	0.01% ± 0.00%	0.02% ± 0.01%	0.02% ± 0.01%
PLA	0.02% ± 0.00%	0.02% ± 0.00%	0.02% ± 0.00%	0.01% ± 0.01%	0.03% ± 0.02%
SSL	0.02% ± 0.00%	0.04% ± 0.01%	0.03% ± 0.00%	0.02% ± 0.01%	0.07% ± 0.04%
POS	1.11% ± 0.07%	1.27% ± 0.07%	1.02% ± 0.04%	1.86% ± 0.24%	1.80% ± 0.24%
OLB	0.05% ± 0.01%	0.04% ± 0.01%	0.05% ± 0.00%	0.04% ± 0.01%	0.05% ± 0.02%
SOG	0.02% ± 0.00%	0.03% ± 0.01%	0.03% ± 0.01%	0.03% ± 0.02%	0.05% ± 0.02%
OOA	0.80% ± 0.05%	0.78% ± 0.05%	0.74% ± 0.02%	1.24% ± 0.19%	0.75% ± 0.11%
PBL	0.00% ± 0.00%	0.01% ± 0.00%	0.01% ± 0.00%	0.00% ± 0.00%	0.01% ± 0.00%
SLA	0.00% ± 0.00%	0.01% ± 0.00%	0.00% ± 0.00%	0.00% ± 0.00%	0.01% ± 0.00%
PPS	0.00% ± 0.00%	0.00% ± 0.00%	0.01% ± 0.00%	0.01% ± 0.00%	0.01% ± 0.00%
OO-21	0.05% ± 0.01%	0.05% ± 0.00%	0.05% ± 0.00%	0.08% ± 0.03%	0.05% ± 0.02%
POA	0.18% ± 0.02%	0.21% ± 0.02%	0.22% ± 0.00%	0.21% ± 0.07%	0.20% ± 0.06%
SSO	0.21% ± 0.02%	0.29% ± 0.02%	0.25% ± 0.01%	0.31% ± 0.09%	0.47% ± 0.15%
OLLg	0.02% ± 0.00%	0.02% ± 0.01%	0.02% ± 0.00%	0.01% ± 0.01%	0.02% ± 0.01%
OOB	0.23% ± 0.02%	0.22% ± 0.02%	0.21% ± 0.01%	0.38% ± 0.14%	0.23% ± 0.08%
PLLg	0.00% ± 0.00%	0.00% ± 0.00%	0.00% ± 0.00%	0.00% ± 0.00%	0.01% ± 0.00%
SLB	0.00% ± 0.00%	0.00% ± 0.00%	0.00% ± 0.00%	0.00% ± 0.00%	0.00% ± 0.00%
OO-23	0.06% ± 0.01%	0.06% ± 0.01%	0.06% ± 0.00%	0.10% ± 0.06%	0.06% ± 0.04%
POB	0.04% ± 0.01%	0.05% ± 0.01%	0.05% ± 0.00%	0.03% ± 0.01%	0.03% ± 0.01%
SOA	0.03% ± 0.00%	0.04% ± 0.00%	0.04% ± 0.00%	0.02% ± 0.01%	0.04% ± 0.01%
OOLg	0.09% ± 0.01%	0.09% ± 0.01%	0.09% ± 0.00%	0.16% ± 0.15%	0.10% ± 0.09%
OO-25	0.04% ± 0.01%	0.04% ± 0.01%	0.04% ± 0.00%	0.07% ± 0.05%	0.04% ± 0.03%
POLg	0.02% ± 0.00%	0.02% ± 0.00%	0.02% ± 0.00%	0.02% ± 0.01%	0.02% ± 0.01%
SOB	0.01% ± 0.00%	0.01% ± 0.00%	0.02% ± 0.00%	0.01% ± 0.00%	0.01% ± 0.01%
OOCe	0.03% ± 0.00%	0.03% ± 0.01%	0.03% ± 0.00%	0.05% ± 0.05%	0.03% ± 0.03%
SOLg	0.00% ± 0.00%	0.01% ± 0.00%	0.01% ± 0.00%	0.00% ± 0.00%	0.00% ± 0.00%
Sum	100.00%	100.00%	100.00%	100.00%	100.00%
DAG/TAG[d]	1.34% ± 0.08%	1.13% ± 0.06%	0.19% ± 0.01%	1.51% ± 0.26%	1.07% ± 0.16%

[a] APCI-MS on high-sensitivity mass spectrometer, TSQ Vantage EMR.
[b] APCI-MS on low-sensitivity mass spectrometer, TSQ 7000.
[c] RF-adjusted ESI-MS data recalculated setting OOL to 10.4%, OOO to 41.0%, and OOP to 20.4% in unadjusted data, assuming charge saturation of these three peaks.
[d] Ratio of total area for diacylglycerols (DAG) versus TAG.

Table 7
Fatty acid (FA) compositions determined by gas chromatography (GC) with flame ionization detection (FID) and calculated from the response factor adjusted diacylglycerol and triacylglycerol compositions of olive oil in dietary supplements determined by APCI-MS, APPI-MS, and ESI-MS.

FA	GC-FID[a] (%)	APCI-MS #1[b] ± SD	APCI-MS #2[c] ± SD	APPI-MS ± SD	ESI-MS ± SD	Sat. Adj. ESI-MS[d] ± SD
M	0.02	0.02% ± 0.00%	0.02% ± 0.00%	0.02% ± 0.00%	0.04% ± 0.01%	0.02% ± 0.01%
Po	0.75	0.76% ± 0.04%	0.77% ± 0.03%	0.77% ± 0.02%	1.08% ± 0.15%	0.76% ± 0.11%
P	11.03	11.07% ± 0.28%	11.10% ± 0.27%	10.55% ± 0.16%	11.59% ± 0.47%	11.06% ± 0.36%
Ln	1.11	1.08% ± 0.02%	1.07% ± 0.07%	1.06% ± 0.02%	1.27% ± 0.08%	1.05% ± 0.06%
L	6.76	6.55% ± 0.12%	6.40% ± 0.25%	6.12% ± 0.06%	6.11% ± 0.18%	6.45% ± 0.19%
O	76.19	76.39% ± 0.59%	76.49% ± 0.63%	77.50% ± 0.21%	74.77% ± 0.51%	76.56% ± 0.53%
S	3.24	3.24% ± 0.09%	3.25% ± 0.12%	3.07% ± 0.05%	3.88% ± 0.28%	3.20% ± 0.22%
A	0.38	0.38% ± 0.03%	0.39% ± 0.02%	0.39% ± 0.01%	0.53% ± 0.07%	0.39% ± 0.05%
G	0.30	0.30% ± 0.02%	0.31% ± 0.02%	0.30% ± 0.01%	0.41% ± 0.08%	0.31% ± 0.06%
21	0.02	0.02% ± 0.00%	0.02% ± 0.00%	0.02% ± 0.00%	0.03% ± 0.01%	0.02% ± 0.01%
B	0.11	0.11% ± 0.01%	0.11% ± 0.01%	0.11% ± 0.00%	0.15% ± 0.04%	0.11% ± 0.03%
23	0.02	0.02% ± 0.00%	0.02% ± 0.00%	0.02% ± 0.00%	0.03% ± 0.02%	0.02% ± 0.01%
Lg	0.05	0.05% ± 0.01%	0.05% ± 0.00%	0.05% ± 0.00%	0.07% ± 0.05%	0.05% ± 0.03%
25	0.01	0.01% ± 0.00%	0.01% ± 0.00%	0.01% ± 0.00%	0.02% ± 0.02%	0.01% ± 0.01%
Ce	0.01	0.01% ± 0.00%	0.01% ± 0.00%	0.01% ± 0.00%	0.02% ± 0.02%	0.01% ± 0.01%
Sum	100.00	100.00%	100.00%	100.00%	100.00%	100.00%

[a] Average of five determinations obtained using AOCS method Ce 1b-89 converted to mole percentage composition.
[b] APCI-MS on high-sensitivity mass spectrometer, TSQ Vantage EMR.
[c] APCI-MS on low-sensitivity mass spectrometer, TSQ 7000.
[d] RF-adjusted ESI-MS data recalculated setting OOL to 10.4%,OOO to 41.0%, and OOP to 20.4% in unadjusted data, assuming charge saturation of these three peaks.

it can be considered to be closest to the "true" FA mole percentage composition.

Comparing Table 7 with Table 5 shows that the error associated with the most abundant FA, oleic acid (O, 18:1), has been reduced from 1.23% absolute (abs), which is 1.61% relative (rel), to 0.18% abs, or 0.23% rel for APCI-MS1, while the difference for APCI-MS2 has been reduced from 2.51% abs (3.30% rel) to 0.28% abs (0.37% rel). More importantly, the difference for linoleic acid (L, 18:2), has been reduced from 1.10% abs (16.34% rel) in Table 5 to 0.21% abs (3.10% rel) for APCI-MS1, and similarly from 1.67% abs (24.77% rel) to 0.36% abs (5.29% rel) for APCI-MS2. Similar improvements can be seen for most FA, and it can be concluded from Table 7 that the RF quantification method of Byrdwell et al. [27] was very effective at adjusting the TAG composition so that the TAG compositions are close to each other for both sets of APCI-MS data, and that the resultant FA compositions match the FA composition by calibrated GC-FID very well.

The DAG composition by APCI-MS is given in Supplemental Table 2, and the resultant FA composition of the DAG is in Supplemental Table 3. As seen in Table 4, the sum of the raw areas of DAG constituted an average of 1.66% between the two APCI-MS instruments, relative to the sum of the raw areas of the TAG. That percentage fell to an average of 1.24% DAG/TAG in Table 6 for the FA RF-adjusted TAG compositions by APCI-MS. Since the FA composition by GC-FID was for the whole oil, which included DAG and TAG, Tables 5 and 7 are for the sum of DAG and TAG. The FA compositions for only the TAG are in Supplemental Tables 4 and 5, for the raw and FA RF adjusted TAG compositions, respectively. The differences between the FA compositions calculated from the TAG plus DAG, versus TAG only FA compositions are negligible.

The fatty acid compositions of olive oil varieties vary widely [29–31]. Almost all FA values in Table 7 are in conformance with the trade standards promulgated by the International Olive Council (IOC) (COI/T.15/NC No 3/Rev. 6, November 2011, www.internationaloliveoil.org), except linolenic acid, which standard is ≤1.0%. The GC-FID value for Ln in Table 7 is 1.11%, and it is not uncommon for some varieties to slightly exceed this value [30,31], especially those in the early ripe stage [30]. Based on the amount of oleic acid, the olive oil in these supplements is much more similar to Italian olive oils [30] than to Argentinean [31] or Spanish [29] varieties. Thus, the results obtained for the olive oil in these dietary supplement samples are in good agreement with literature precedent for olive oil FA compositions and with IOC trade standards for all but Ln.

Holcapek and Lisa [32] and Fasciotti and Netto [33] have reported quantitative analysis of olive oil TAG using LC-APCI-MS. Holcapek and Lisa [32] showed a very similar set of TAG, including those with very long-chain FA (VLCFA) up to 26:0 and odd-chain FA in their Fig. 1. The weight percentage FA composition in that report was calculated from a subset of those TAG. Based on the high variability for different varieties of olive oil described by the reports above and the IOC standards, and the fact that the specific varieties of olive oil are not given for the dietary supplements or in the other reports of APCI-MS of olive oil TAG, there is no reason to expect that the TAG and FA compositions should be the same for the olive oil compositions given in the different reports. Nevertheless, for the sake of thoroughness, the FA composition reported by Holcapek and Lisa [32], converted to mole percentage by dividing by the weight of the FAME and normalized to 100% (these made up 99.8% of FA by weight), is as follows: Po: 1.4%; P: 13.6%; Ln: 1.0%; L: 6.5%; O: 74.1%; S: 2.3%; A: 0.4%; G: 0.4%; B: 0.2%; Lg: 0.1%. This can be compared to the un-normalized results in Table 5, where this subset made up 99.92% of our mole percentage composition. Given the lack of common GC-FID data, and no expectation that these are the same or similar olive oil varieties, there is no basis for additional detailed comparison.

In addition to the primary peaks arising from $[DAG]^+$ fragments and the $[M+H]^+$, both the new and older APCI-MS instruments produced similar adducts at $[M+54]^+$, $[M+55]^+$, $[M+90]^+$, and $[M+124]^+$ arising from chemical ionization of acetonitrile and dichloromethane in the ionization source. The $[M+55]^+$ adduct ion is slightly more abundant than an accompanying $[M+54]^+$ adduct (small peaks at *m/z* 936.8, 937.8 visible in Fig. 3D and 3H but not labeled). A *m/z* 54 ion from ACN has been proposed to be $CH_2=C=N^+=CH_2$ [34], $C_3H_4N^+$, which has been used to great effect by Brenna and colleagues for covalent adduct chemical ionization MS for double bond localization [35–37]. None of those works conclusively identify the $[M+55]^+$ often seen in APCI-MS spectra (the $[M+55]^+$ in [34] has a ^{13}C). It is possible that the $[M+55]^+$ could be an odd-electron variant of the above ion, $CH_2=C=N^{\cdot+}-CH_3$, or similar $C_3H_5N^+$ isomer, or an even-electron species such as $CH_2=N-N^+\equiv CH$, or a similar $C_2H_3N_2^+$ isomer. But in the absence of isotope labeled experiments, there is no foundation to specify its identity here. The $[M+90]^+$ and $[M+124]^+$ adducts have isotopic distributions that indicate the presence of

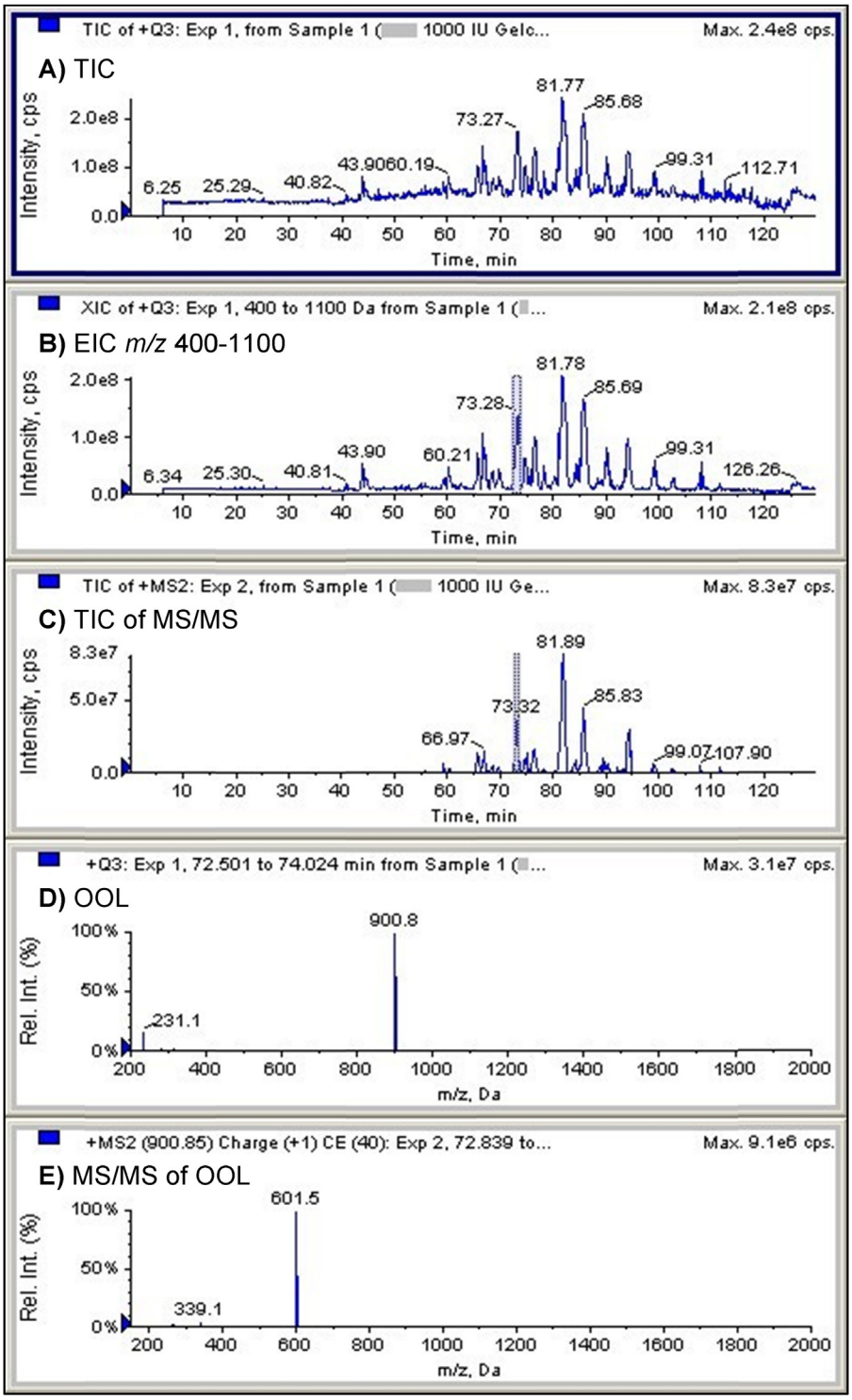

Fig. 5. Electrospray ionization (ESI) MS chromatograms and spectra from olive oil filled gelcap, with ammonium formate electrolyte added via tee. A) Total ion current chromatogram (TIC) of ESI-MS; B) extracted ion chromatogram (EIC) of the range *m/z* 400–1100; C) TIC of MS/MS scans; D) average mass spectrum across OOL peak at 73.3 min; E) MS/MS spectrum of *m/z* 900.8. Sample identity masked.

chloroform, implicating a reaction between the ACN and DCM mobile phase solvents. The $[M+90]^+$ and $[M+124]^+$ adduct ions appear straightforward to identify as $CH_3{-}C{\equiv}N^+{-}CH_2Cl$ (or isomer) for *m/z* 90 and $CH_3{-}C{\equiv}N^+{-}CHCl_2$ (or isomer) for *m/z* 124. In addition to these adducts, the APCI-MS mass spectra also exhibit the $[M+H{-}H_2O]^+$ dehydration product typical of APCI-MS spectra.

3.4. TAG and FA compositions by APPI-MS

One of the many advantages of the multiple parallel mass spectrometry approach is that it allows direct comparison between ionization techniques run on the same sample at the same time, which makes differences between techniques more apparent. One trend that became immediately obvious from Table 4 was that

APPI-MS favored polyunsaturated FA-containing TAG even more than APCI-MS. Almost every early-eluting TAG that contained Ln or L gave a higher percentage composition by APPI-MS than by either of the two APCI-MS instruments. This trend for TAG can be summarized by OOL and OOP. OOL eluted before OOO and gave a percentage of 15.01% by APPI-MS compared to 10.41% and 10.35% by APCI-MS 1 and 2, respectively, whereas OOP eluted after OOO and gave a percentage of 13.42% by APPI-MS, compared to 20.90% and 19.91% by APCI-MS 1 and 2, respectively. This can also be seen from the larger early-eluting peaks and smaller late-eluting peaks in the chromatogram in Fig. 3K, when compared to Fig. 3B and G. This trend was borne out in Table 5, which shows higher percentages of Ln and L in the FA composition calculated from the TAG composition from APPI-MS.

This trend did not seem to be the case in the report by Cai et al. [10], who showed peaks for injections of mixtures of 1 μg/mL of Type I and Type II TAG, in which SSO appeared to give the largest peaks. However, different peak sizes in that report, based on different mobile phases, and differences between the instrument and conditions used there and those employed here indicate that a variety of factors affect response by APPI. Nevertheless, the different peak sizes for the same amounts of analyte in that earlier report [10] clearly indicate different response by APPI-MS to TAG having different degrees of unsaturation.

APPI-MS has been shown to exhibit large differences in response from different solvents [8], with acetonitrile being one of solvents that produced the least response, whereas dichloromethane produced good response. Thus, it could be expected that in the gradient with DCM and ACN, as the DCM percentage increased, the signal would increase. But the difference in response due to unsaturation appears to be the dominant factor, since early-eluting polyunsaturated peaks that gave larger signal eluted during the part of the gradient that had a higher percentage of ACN and lower percentage of DCM.

To compensate for such factors, the method of Byrdwell et al. [26,27] was applied to the TAG composition from APPI-MS, and the agreement to the APCI-MS results was dramatically improved for most of the TAG, with the exception of OOO. The percentage of OOO happened to agree quite well in the non-RF-adjusted compositions. But as the FA composition in Table 5 showed, all FA compositions calculated from API-MS methods were too low for O, compared to calibrated GC-FID. For L and Ln, which showed substantially higher values by APPI-MS than those from APCI-MS, the FA values obtained after application of the method of Byrdwell et al., shown in Table 7, were in much better agreement between APPI-MS, APCI-MS, and GC-FID. The differences between the FA compositions by GC-FID and by APPI-MS for the three largest FA (O, P, and L) were initially 3.66% abs (4.81% rel) for O, 3.22% abs (29.19% rel) for P, and 5.72% abs (84.56% rel) for L. These were reduced to 1.31% abs (1.72% rel) for O, 0.48% abs (4.36% rel) for P and 0.64% abs (9.44% rel) for L. The average error for FA present at ≥0.3% was reduced from 43.31% rel to 4.10% rel, indicating that this approach to RF calculation was very effective and reducing the error between the FA percentage calculated from APPI-MS and that determined from calibrated GC-FID, as well as reducing the differences in Table 6 between TAG compositions by APCI-MS and APPI-MS.

Fig. 3K, compared to Fig. 3B and G, showed only small peaks for DAG between 40 and 50 min, which were similarly smaller in the EIC. The lower response to DAG compared to APCI-MS is reflected in the DAG/TAG ratio calculated from the raw DAG and TAG areas, given at the bottom of Table 4. The DAG composition is given in Supplemental Table 2, and as expected, the DAG also reflected the greater response of polyunsaturated DAG, similar to the behavior of TAG, although the overall response of DAG was lower than by the other API techniques.

For TAG, APPI-MS did appear to have some benefits over APCI-MS. APPI-MS required the use of a dopant (acetone) to obtain maximum signal, but with that caveat, it appeared to produce larger signal than APCI-MS, and produced fewer of the adducts mentioned above for APCI-MS. Furthermore, since APPI is a non-contact ionization process (i.e. there is no corona needle for residue to build up on), cleanup between sequences was easier on the APPI-MS instrument. Although it is not fair to compare the raw signals obtained on the different instruments, since they depend on tuning parameters and electron multiplier voltage, etc., it is appropriate to compare the %RSD in the signals. It can be noted that the APPI-MS instrument produced the largest raw areas for OOO, but had a %RSD in those areas of 13.1%. This was nearly the same as APCI-MS1, which had a %RSD of 13.0% in the raw OOO areas. APCI-MS2 had a %RSD of 6.3%RSD, while the ESI-MS instrument gave a % RSD of 3.8% for the OOO areas. The OOO areas by APPI-MS showed a decrease in signal over the course of the sequence, similar to that observed for APCI-MS, while ESI-MS did not show a distinct downward trend. Our results on these four different instruments for overall signal intensity and mass spectral quality are in general agreement with the report by Cai and Syage [9] that showed some benefit to APPI-MS over APCI-MS that was acquired on the same instrument.

Unfortunately, APPI-MS on this instrument did not respond sufficiently well to vitamin D to allow qualitative or quantitative identification of those peaks. Quantification of vitamin D was a crucial component of this analysis of dietary supplements. Thus, while APPI-MS proved to be a valuable complement to APCI-MS for TAG analysis, it could not be used as the sole detection technique for this analysis under the conditions used here. This chromatographic system was not optimized for APPI-MS, but rather was optimized for separation of vitamin D and TAG, and the MS techniques were required to perform under those conditions. Furthermore, APPI-MS was performed on the quadrupole ion trap MS instrument (versus a linear trap or hybrid trap), so only the least sensitive approach, EIC, could be used, instead of a more sensitive SRM method. Also, note that the APPI source was contaminated with the ESI-MS electrolyte normally used on that instrument, and after disassembling and cleaning the source, a small amount of ammonium adduct was still visible in the mass spectra, such as Fig. 3N.

The larger effect due to unsaturation for APPI-MS compared to APCI-MS highlights the importance of obtaining the FA composition by calibrated GC-FID or similar independent calibrated method for determination of the FA composition. We have in the past, as have most researchers who report API-MS analysis of TAG, reported TAG compositions by LC-MS without providing the accompanying GC-FID FA compositions. The quadruple parallel MS technique, which allows direct comparison between instruments, makes the need for both types of data more apparent. Fortunately, the method of Byrdwell et al. for quantification provides a straightforward solution to compensate for the dependence of TAG spectra, and corresponding percentage composition, on the degree of unsaturation and carbon chain length.

3.5. TAG and FA compositions by ESI-MS

As mentioned above, ionization sources from different manufacturers behave differently, and different versions of sources from the same manufacturer show differences. The fragment ratios are also affected by tuning and optimization parameters. The ESI source on the QTrap 4000 instrument produced a lower S/N in TIC than we previously reported using ESI-MS on an LCQ Deca XP instrument [19], as seen in Fig. 5. Furthermore, the source on the QTrap was more prone to charge saturation due to overpopulation of ions in the source [38] than was the instrument used previously, under similar optimized conditions using the same electrolyte solution. In the past, we were able to analyze mixtures of TAG up to

as high as 5–10 mg/mL without difficulty. It was apparent from Table 4 that these gelcaps, which gave ~1 mg/mL solutions using the dilute-and-shoot approach, overwhelmed the source for the most abundant TAG, OOO, giving a much lower percentage by ESI-MS on this instrument than by the other API-MS techniques. Furthermore, OOP and OOL can also be seen to under-respond. Other L-containing TAG in Table 4 gave larger percentages than by APCI-MS, but OOL gave a slightly smaller response, indicating that the tendency toward increased response due to the degree of unsaturation was more than offset by signal suppression due to charge saturation. Fig. 5 shows that the three largest peaks are not as large relative to the neighboring peaks as they are in Fig. 3 for APCI-MS and APPI-MS. The cutoff for peaks that led to charge saturation appears to be between POL, present at 6.71%, which responded more than both APCI-MS and APPI-MS, and OOL, present at 9.88%, which responded less. Thus, the phenomenon appears to be limited to the three most abundant TAG, OOO, OOP, and OOL. The dependence of response of ESI-MS due to the degree of unsaturation was reported in some of the earliest reports of ESI-MS of TAG [39,40], and similarly the effect of acyl chain length, degree on unsaturation and other factors has been well documented for phospholipids [41].

Of course, the under-response of the most abundant oleic acid-containing TAG is reflected in the FA composition in Table 5, which shows a substantially lower value for O by ESI-MS than by GC-FID and by the other API-MS techniques.

If we recognize from Table 4 that the three most abundant TAG (OOO, OOP, and OOL) under-responded, probably due to charge saturation in the source, there is a limited number of options to deal with the data. We could ignore the ESI-MS results, since they are clearly compromised, and we could consider the remaining triple parallel mass spectrometry results adequate. This is a perfectly viable option, since Tables 6 and 7 show four sets of data (GC-FID, 2xAPCI-MS and APPI-MS) that agree well and provide a good indication of the TAG and FA compositions of the oil in these supplements.

Alternatively, we could assume reasonable values for the three charge-saturated molecular species based on the other API-MS techniques acquired at the same time as the ESI-MS data, and then re-normalize the data including the three estimated values. The latter approach is similar to the technique demonstrated previously, when three TAG (SSS, SSP, and PPS), referred to as the "hard stocks" since they increased the solid fat content of the mixtures, were blended with TAG base stocks (corn oil, canola oil, and soybean oil) to give TAG mixtures with improved performance characteristics [27]. Based on knowledge of the composition of the hard stock, including the composition by GC-FID and knowledge of the blend ratio, we were able to develop the "blend modification" of the Byrdwell et al. method [27]. Although the conditions are different, the principles are similar, and thus the blend modification of the Byrdwell et al. method can be adapted and applied to the ESI-MS data.

We can multiply the three under-responding TAG (OOO, OOP, OOL) by factors that, when the TAG composition is re-normalized to 100%, give the average values obtained from APCI-MS (APCI-MS is used since both values agree very well). This is a conservative approach that underestimates the over-response of OOL, since the dependence on unsaturation was less by APCI-MS than ESI-MS, judging from the percentages for other Ln- and L-containing TAG. If we multiply the raw areas for OOO times 4.800236, OOP times 2.829705, and OOL times 2.145492 (extra decimal places used to minimize rounding error) and re-normalize the sum to 100%, we obtain the saturation-adjusted TAG composition given in Table 4 in the column "Sat. Adj. ESI-MS". This composition now has OOO, OOP, and OOL equal to the average values from the two APCI-MS instruments, 41.0%, 20.0%, and 10.4%, respectively. No other RF have been applied; this is simply an initial step to compensate for charge saturation of the three most abundant TAG molecular species. A seen in Table 5, the agreement to the FA composition by GC-FID and by APCI-MS has been greatly improved, while still reflecting the natural over-response arising from Ln- and L-containing species. Both Ln and L are still larger than by APCI-MS, but by a smaller amount than originally, reflecting the slightly greater over-response to unsaturated species by ESI-MS versus APCI-MS. The average difference to the GC-FID composition, for FA $\geq$0.3%, has been reduced from 4.51% abs (110.51% rel) to 0.90% abs (21.89% rel). Most of the error was attributable to Ln, L, Po, and G, in order of decreasing % error. Table 4 shows that the TAG composition by saturation-adjusted ESI-MS, before application of the normal Byrdwell et al. RF method, is much closer to the raw TAG compositions obtained by APCI-MS, while still reflecting the larger response of polyunsaturated TAG. In many, but not all, cases the saturation-adjusted TAG composition by ESI-MS shows larger percentages for polyunsaturated TAG than by APCI-MS, but less than by APPI-MS.

The FA RF approach was then applied to the saturation-adjusted raw ESI-MS TAG composition as usual, resulting in the TAG composition given in Table 6 in the column "Sat. Adj. ESI-MS". Table 6 shows that the saturation-adjusted FA RF-adjusted ESI-MS composition is in fairly good agreement to the other API-MS techniques. As we stated in our previous report [27]: "The method of calculation of response factors developed by us applies FA response factors evenly to all TAG containing a particular fatty acid. The calculation method makes the assumption that the over- or under-response of a fatty acid results from all of the TAG which contain that fatty acid. Oil blends with hard stocks do not obey this assumption. In vegetable oil with hard stocks blends, a few specific TAG contributed almost all of the stearic acid and much of the palmitic acid present." In a similar fashion, charge saturation of the most abundant three TAG was responsible for most of the under-response of O in the dietary supplements. Therefore, the charge saturation variation of the blend modification of the Byrdwell et al. method was successful in compensating for the under-response by using a similar two step approach. First, the three TAG that underwent charge saturation were set to reasonable conservative values determined from APCI-MS, allowed by the quadruple parallel MS approach. Second, the FA RF approach was applied to all TAG, as usual.

If the FA RF approach is used without first compensating for the charge saturated species, the RF for O is larger, to compensate for the low values for OOO, OOP, and OOL. This makes the TAG percentages for oleic acid-containing TAG other than OOO, OOP, and OOL generally too large, while those three TAG are still too low, as seen in Table 6 for the ESI-MS results that were not saturation-adjusted. This effect was offset to some extent by Ln- and L-containing TAG, since those RF were larger.

The FA composition calculated from the TAG composition in Table 7 shows much better agreement to the GC-FID FA composition compared to Table 5. While the non-saturation-adjusted FA composition in Table 7 also shows better agreement, the saturation adjusted FA composition is superior. The agreement to the "true" FA composition is outstanding for the FA compositions calculated from the saturation-adjusted ESI-MS and both APCI-MS TAG compositions, and the agreement of the APPI-MS values is also very good. Thus, Table 7 indicates that the FA RF method and the charge saturation variation of the blend modification of the FA RF method have brought all values to a unified consensus around the values obtained by calibrated GC-FID.

3.6. TAG and FA compositions by CAD and ELSD

Table 4 shows that only TAG present at a level of ~$\geq$0.6% (~120 ng) were quantifiable in the CAD chromatograms, Fig. 1D, and an even smaller subset of those could be detected by ELSD, Fig. 1B. Table 4 and Fig. 1D also show that the CAD dramatically

over-responded to DAG, and gave a DAG/TAG of 22%, compared to 1.66% and 1.24% averages by APCI-MS before and after applying FA RF. Conversely, the ELSD gave a small peak for only one DAG (OO1), showing only 0.08% DAG/TAG, because DAG were present at low levels. Overall, the CAD and ELSD were found to be inadequate for TAG analysis of the 1 mg/mL solution under the conditions used. Newer models of ELSD may be more useful, whereas the Corona CAD was recently upgraded.

4. Conclusion

The data herein demonstrated multiple novel advancements, including:

- The first report of the use of four mass spectrometers simultaneously, using three different API techniques, for a "quadruple parallel mass spectrometry" approach.
- A meta-analysis of vitamin D analyses over two months, to provide a much better indication of the reliability of the method, compared to the single sequence results presented previously [7].
- Vitamin D from lanolin was found to not contain interfering TAG species such as those that were observed from vitamin D 'molecularly distilled' from fish oil [7].
- The inclusion of the $1 \times {}^{13}C$ for TAG quantification to increase usable signal by ~ 30-50%, without loss of specificity.
- The first application of the Byrdwell et al. method [26] to APPI-MS data, showing that it was equally effective as it was for APCI-MS.
- The charge saturation variation of the blend modification of the Byrdwell et al. method [27] allowed ESI-MS data to be salvaged by compensating for the effects of charge saturation of the three most abundant TAG, by assigning conservative, reasonable values based on APCI-MS data in parallel.

These data also confirmed and expanded our previous results for vitamin D and TAG, allowing us to conclude:

- UV at 265 nm data had lower sample-to-sample % RSD than MS results in all cases.
- Vitamin D iRF results are as accurate and precise as calibration curve results, if the standard used to determine the iRF is close to the sample analyte concentration, but error increased for iRF results as the standard concentration diverged from the analyte concentration.
- ES results by MS had higher % RSD than IS and iRF results.
- SIM gave higher signal than SRM, and equivalent results to SRM1, but with less specificity.
- SRM2 gave slightly higher values and higher % RSD than SIM and SRM1.
- The Byrdwell et al. method for quantification using RF calculated from the GC-FID FAME composition was very effective at compensating for discrimination based on degree of unsaturation and other factors, leading to FA RF adjusted values that agreed well across all API-MS techniques and GC-FID.
- Since quadruple parallel mass spectrometry may not be widely accessible, a minimum configuration of LC-MS with UV detection and APCI-MS could be used, since APCI-MS gives good response to both vitamin D and TAG.
- The FA composition from TAG by LC-MS should always be compared to that by GC-FID, since response by all API techniques are affected by the degree of unsaturation in TAG, as well other factors.
- Based on the unique characteristics of each instrument, it would be more beneficial to perform ESI-MS of TAG on the LCQ Deca XP instrument, as previously reported, and perform APPI-MS on the QTrap 4000 instrument.

Acknowledgment

This work was supported by the USDA Agricultural Research Service. Mention or use of specific products or brands does not represent or imply endorsement by the USDA. The work of Brian Nies of Morpho Detection, Inc. (formerly Syagen Technologies, Inc.) to refurbish the APPI source for the LCQ Deca XP instrument is gratefully acknowledged. The work of Dr. Robert Goldschmidt to perform GC FAME analyses and UV, CAD and ELSD peak integration is gratefully acknowledged.

Appendix A. Supplementary data

Supplementary data associated with this article can be found, in the online version, at http://dx.doi.org/10.1016/j.chroma.2013.10.031.

References

[1] I. Marchi, S. Rudaz, M. Selman, J.L. Veuthey, J. Chromatogr. B Anal. Technol. Biomed. Life Sci. 845 (2007) 244.
[2] A. Vaikkinen, B. Shrestha, T.J. Kauppila, A. Vertes, R. Kostiainen, Anal. Chem. 84 (2012) 1630.
[3] R.R. Eitenmiller, W.O. Landen, Vitamin Analysis for the Health and Food Sciences, CRC Press, Boca Raton, FL, 1999.
[4] J. Exler, K.M. Phillips, K.Y. Patterson, J.M. Holden, J. Food Comp. Anal. 29 (2013) 110.
[5] M. Huang, D. Winters, D. Sullivan, D. Dowell, J. AOAC Int. 95 (2012) 319.
[6] F. Granado-Lorencio, C. Herrero-Barbudo, I. Blanco-Navarro, B. Pérez-Sacristán, Anal. Bioanal. Chem. 397 (2010) 1389.
[7] W.C. Byrdwell, Anal. Bioanal. Chem. 401 (2011) 3317.
[8] S.S. Cai, J.A. Syage, J. Chromatogr. A 1110 (2006) 15.
[9] S.S. Cai, J.A. Syage, Anal. Chem. 78 (2006) 1191.
[10] S.S. Cai, L.C. Short, J.A. Syage, M. Potvin, J.M. Curtis, J. Chromatogr. A 1173 (2007) 88.
[11] J.L. Gomez-Ariza, A. Arias-Borrego, T. Garcia-Barrera, R. Beltran, Talanta 70 (2006) 859.
[12] W. Herchi, H. Trabelsi, H.B. Salah, Y.Y. Zhao, S. Boukhchina, H. Kallel, J.M. Curtis, Afr. J. Biotechnol. 11 (2012) 904.
[13] L. Imbert, M. Gaudin, D. Libong, D. Touboul, S. Abreu, P.M. Loiseau, O. Laprévote, P. Chaminade, J. Chromatogr. A 1242 (2012) 75.
[14] I. Marchi, S. Rudaz, J.L. Veuthey, Talanta 78 (2009) 1.
[15] J. Cvacka, E. Krafkova, P. Jiros, I. Valterova, Rapid Commun. Mass Spectrom. 20 (2006) 3586.
[16] W.C. Byrdwell, R.H. Perry, J. Chromatogr. A 1133 (2006) 149.
[17] W.C. Byrdwell, J. Exler, S.E. Gebhardt, J.M. Harnly, J.M. Holden, R.L. Horst, K.Y. Patterson, K.M. Phillips, W.R. Wolf, J. Food Comp. Anal. 24 (2011) 299.
[18] W.C. Byrdwell, Rapid Commun. Mass Spectrom. 12 (1998) 256.
[19] W.C. Byrdwell, W.E. Neff, Rapid Commun. Mass Spectrom. 16 (2002) 300.
[20] W.C. Byrdwell, Lipids 40 (2005) 383.
[21] M. Holcapek, M. Lisa, P. Jandera, N. Kabatova, J. Sep. Sci. 28 (2005) 1315.
[22] P. Laakso, J. Am. Oil Chem. Soc. 74 (1997) 1291.
[23] P. Laakso, P. Voutilainen, Lipids 31 (1996) 1311.
[24] H.R. Mottram, R.P. Evershed, Tetrahedron Lett. 37 (1996) 8593.
[25] M. Holcapek, H. Dvorakova, M. Lisa, A.J. Giron, P. Sandra, J. Cvacka, J. Chromatogr. A 1217 (2010) 8186.
[26] W.C. Byrdwell, E.A. Emken, W.E. Neff, R.O. Adlof, Lipids 31 (1996) 919.
[27] W.C. Byrdwell, W.E. Neff, G.R. List, J. Agric. Food Chem. 49 (2001) 446.
[28] W.C. Byrdwell, E.A. Emken, Lipids 30 (1995) 173.
[29] L. Leon, M. Uceda, A. Jimenez, L.M. Martin, L. Rallo, Spanish J. Agric. Res. 2 (2013) 353.
[30] M. Poiana, A. Mincione, Grasas Aceites 55 (2004) 282.
[31] D.P. Rondanini, D.N. Castro, P.S. Searles, M.C. Rousseaux, Grasas Aceites 62 (2011) 399.
[32] M. Holcapek, M. Lisa, Lipid Technol. 21 (2009) 261.
[33] M. Fasciotti, A.D. Pereira Netto, Talanta 81 (2010) 1116.
[34] H. Wincel, R.H. Fokkens, N.M.M. Nibbering, Int. J. Mass Spectrom. Ion Processes 96 (1990) 321.
[35] C.K. Van Pelt, B.K. Carpenter, J.T. Brenna, J. Am. Soc. Mass Spectrom. 10 (1999) 1253.
[36] C.K. Van Pelt, J.T. Brenna, Anal. Chem. 71 (1999) 1981.
[37] Y. Xu, J.T. Brenna, Anal. Chem. 79 (2007) 2525.
[38] K. Tang, J.S. Page, R.D. Smith, J. Am. Soc. Mass Spectrom. 15 (2004) 1416.
[39] C. Cheng, M.L. Gross, E. Pittenauer, Anal. Chem. 70 (1998) 4417.
[40] K.L. Duffin, J.D. Henion, J.J. Shieh, Anal. Chem. 63 (1991) 1781.
[41] M. Koivusalo, P. Haimi, L. Heikinheimo, R. Kostiainen, P. Somerharju, J. Lipid Res. 42 (2001) 663.